52p

NASA TN D-1661

N63-15695
Code-1

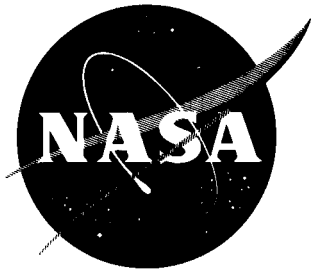

TECHNICAL NOTE

D-1661

DESIGN AND OPERATIONAL PERFORMANCE OF A 150-KILOWATT SODIUM FLASH-VAPORIZATION FACILITY

By Landon R. Nichols, Charles H. Winzig,
Stanley M. Nosek, and Louis J. Goldman

Lewis Research Center
Cleveland, Ohio

NATIONAL AERONAUTICS AND SPACE ADMINISTRATION
WASHINGTON

May 1963

55446

58p

NATIONAL AERONAUTICS AND SPACE ADMINISTRATION

TECHNICAL NOTE D-1661

DESIGN AND OPERATIONAL PERFORMANCE OF A 150-KILOWATT SODIUM FLASH-VAPORIZATION FACILITY

By Landon R. Nichols, Charles H. Winzig,
Stanley M. Nosek, and Louis J. Goldman

15695

SUMMARY

The mechanical, electrical, and process design, and the operational performance of a 150-kilowatt sodium flash-vaporization facility are presented. Saturated liquid sodium at temperatures to 1600° F was circulated at flow rates to 19,000 pounds per hour through an electric-resistance heater. A maximum heater-outlet temperature of 1700° F is attained prior to decompression of the liquid to allow fractional flash vaporization. The liquid-vapor mixture is separated centrifugally, the saturated liquid is recirculated, and the saturated vapor is passed through a convergent nozzle, which simulates a turbine.

A maximum vapor flow of 300 pounds per hour is passed to an air-cooled condenser, which is operated at condensing temperatures to 1550° F. The saturated condensate is compressed and mixed with the separator liquid effluent.

Stable system operation is realized throughout the range of design parameters. No process instabilities occurred in the flashing process during either transient or steady-state operation. Tentative restricted and critical-flow data of sodium vapors through a convergent nozzle are presented and are compared with theoretically predicted flow for supersaturated and equilibrium expansions.

An account of the operational problems, process characteristics, and process interruptions encountered during the 800-hour performance run are presented.

INTRODUCTION

Manned vehicles for space travel and exploration will require power systems in the megawatt range. Such systems must be reliable for long periods of time, perhaps a few years, and should demand little maintenance to sustain design performance. Nuclear heat appears to be the best source of energy for the power levels needed for propulsion and operation of manned space power vehicles.

The conversion of nuclear energy to electric power can be attained indirectly by turbine-generator units operating in a closed thermodynamic gas or vapor cycle. Heat is added to the working substance from the energy source, and waste heat is rejected from the working fluid by radiation to the space environment. The Rankine vapor cycle using an alkali metal as the working fluid is

promising for use in a manned space power system. The gross weight of these systems must be minimized without jeopardizing long-term reliability.

The indirect conversion of nuclear energy to electric power for ion propulsion has been the subject of numerous analytical studies. Reference 1 discusses a conceptual nuclear turboelectric manned space vehicle. Here the authors recognized many areas where pronounced advances in engineering science must be accomplished before such a vehicle could become a reality. The optimization of the weight of a space radiator with reference to the efficiency of the power cycle has been discussed in references 2 and 3. These studies are not conclusive for space application because of the lack of engineering information on such advanced systems.

Current engineering knowledge and practice, and forseeable advances in basic and applied engineering, indicate that alkali-metal systems exhibiting long-term reliability at temperatures as high as 2200° F will be among the first generation of manned space power systems. An effort is now under way at both government and industrial laboratories to advance rapidly the technology of liquid metals at these higher temperatures. At the NASA Lewis Research Center, particularly, experimental work is proceeding (1) to develop new materials of construction and fabrication techniques compatible with the alkali metals; (2) to investigate the phenomena associated with heat transfer to the alkali metals during vaporization and condensation; (3) to develop durable and efficient rotating components, that is, turbines and pumps; and (4) to investigate system control and general operational problems by the operation of integrated pilot facilities.

A summary of the design and operational performance of a pilot facility with sodium as the working substance is made herein. The forced-circulation liquid-vapor alkali-metal system consists of two main interconnected processes. The primary system is used to investigate the feasibility of generating saturated metallic vapor by the flash vaporization of compressed liquid sodium and subsequent separation of the saturated phases. Particular interest is directed to possible process instabilities introduced by the large variation of vapor pressure with temperature of the alkali metals. The secondary system is used to study the expansion and flow characteristics of saturated sodium vapor. The vapor is passed through a nozzle to obtain critical weight-flow information and to study the expansion process through a convergent nozzle. Such information is of both theoretical and practical interest in the design and the operation of vapor turbines. The facility affords the opportunity to familiarize personnel with the general operation of two-phase liquid-metal systems and provides a dynamic system for evaluation of instrumentation components. From such an operation, component and general process reliability and durability data are also obtained.

An account of the operational problems and characteristics of the system processes are presented herein. Problems encountered in the control and instrumentation of the system, including measurement of pressure, flow, and liquid level, are discussed. Operational methods and process safety devices are included. Finally, a statement is given of the modifications to be made to the system to improve the general performance; a brief discussion of the use of the system for basic research and testing of liquid-metal-system components is presented.

SYMBOLS

A	area, sq in.
C_p	molal specific heat at constant pressure, Btu/(lb-mole)(^oR)
C_v	molal specific heat at constant volume, Btu/(lb-mole)(^oR)
h	specific enthalpy, Btu/lb
J	mechanical equivalent of heat, 778.2 ft-lb/Btu
M	molecular weight, lb
p	absolute pressure, lb/sq in.
R	universal gas constant, 1545 ft-lb/(lb-mole)(^oR)
s	specific entropy, Btu/(lb)(^oR)
T	absolute temperature, ^oR
V	velocity, ft/sec
v	specific volume, cu ft/lb
w	weight-flow rate, lb/hr
X	mole fraction
x	quality, lb vapor/lb mixture
γ	ratio of specific heats

Subscripts:

c	critical
f	liquid
g	vapor
m	mixture
Na_1	monatomic sodium vapor
Na_2	diatomic sodium vapor
o	initial-state point
p	primary system

s	secondary system
t	nozzle throat
x	variable-state point
1	heater outlet, orifice inlet
2	separator inlet
3	separator vapor outlet, nozzle inlet
3'	separator liquid outlet
4	nozzle outlet
5	condenser inlet
6	condenser outlet
6'	accumulator outlet
7	secondary-pump outlet
8	primary-pump inlet
9	primary-pump outlet, heater inlet

DESCRIPTION OF SYSTEM

Thermodynamic Cycle

The thermodynamic cycle of the sodium flash-vaporization system is shown in the enthalpy-entropy diagram in figure 1(a). Figure 1(b) indicates the principal components of the system; thermodynamic processes are bounded by the noted state points.

Subcooled liquid at state 1 is depressurized by flowing through an orifice; a fraction of the liquid vaporizes, and the two-phase mixture, state 2, flows to the separator. Saturated vapor from the separator, state 3, is expanded through a convergent nozzle to state 4. In the vapor environmental chamber, the velocity head is converted to enthalpy, and superheated vapor, state 5, results. Desuperheating and condensing provide saturated liquid, state 6. Heat losses from the accumulator result in subcooled condensate, state 6'. This condensate is compressed by the secondary pump to state 7 and mixed with the saturated liquid from the separator, state 3', which locates a slightly subcooled liquid, state 8. Compressed liquid from the primary pump, state 9, is heated prior to flashing from state 1 to complete the cycle.

Design Criteria

The sodium flash-vaporization system is designed to circulate up to 50 gallons per minute (19,000 lb/hr) of sodium in the primary circuit. The discharge of the primary pump at temperatures to 1620° F is passed through the main heater where a maximum of 150 kilowatts of power is added to the sodium by electric-resistance heating. Eighty-five percent of the heat is generated directly in the flowing liquid; the remainder is generated in the process pipe by impressing up to 18 volts and 10,000 amperes single-phase alternating current to the main heater pipe. The maximum temperature of the sodium at the heater outlet at peak design is 1700° F. A concentric orifice is located at the main heater outlet, which allows compression of the liquid sodium to prevent boiling within the heater. Decompression of the liquid, due to flow through the orifice, allows flash vaporization of a fraction of the liquid sodium at a maximum vapor-generation rate of 300 pounds per hour. The two-phase mixture is separated in a centrifugal separator from which the liquid is recirculated through the primary system, and the vapors pass overhead from the separator to a convergent nozzle that limits the sodium-vapor mass-flow rate to the condenser. The air-cooled condenser is sized to condense up to 300 pounds per hour of sodium vapors at temperatures to 1620° F. The condensate is compressed and mixed with the saturated liquid from the separator. During operation, the process system contains 200 pounds of sodium.

Mechanical

The two-phase sodium facility is composed of three process subsystems: (1) primary, (2) secondary, and (3) oxide control and indicating. The auxiliary systems are: (1) sump tank, (2) evacuation and inerting system, and (3) liquid sampling. Schematic and isometric drawings of the facility are shown in figures 2 and 3, respectively. Figure 4(a) shows the facility during construction. All process piping is AISI 316 seamless stainless steel, schedule 40 (except as elsewhere noted) with butt-welded joints. The vessels within the system are fabricated from pipe sections with standard ASME butt-welded head closures. There are six packless bellows-sealed valves in the system, of which only the valve in the secondary system is operated under high-severity conditions. All welds are made by the tungsten inert-arc process and are dye penetrant and radiographically inspected. The entire facility is leak checked by using a helium mass spectrometer.

An $8\frac{1}{2}$- by $13\frac{1}{2}$- by $11\frac{1}{2}$-foot steel enclosure with removable panels and hinged access doors (fig. 4(b)) houses and supports the piping and components. All vessels and the tee connecting the primary and secondary systems are anchored to the framework of the enclosure. Straight runs of structural steel, securely strapped to the underside of the thermal insulation, are welded to the framework to provide vertical support to the main heater. Steel cables support the piping vertically and allow lateral movement from thermal growth, while suitable bends and loops are provided to relieve the thermal stresses. Adjustable spring-loaded cables provide proper support for the primary pump and the valve actuators under varying structural loads. All process piping and vessels are covered with 5 inches of high-temperature thermal insulation.

Primary system. - The sodium from the liquid-vapor separator flows through a flowmeter to the primary pump, the main heater, an orifice, and back into the separator to complete the cycle.

The separator, which operates on the centrifugal or cyclone principle, is 14 inches in diameter and 48 inches long. During operation, an inventory of about 1 cubic foot of liquid is maintained in the separator to ensure a positive suction head to the primary pump. The vapor passes from the top of the vessel into the secondary system, whereas the liquid, draining from the bottom, flows through a $2\frac{1}{2}$-inch-diameter pipe to a junction where it combines with the condensate from the secondary system. The combined streams then flow through the flowmeter.

The magnetic flowmeter is located upstream of the primary pump, contrary to convention, to remove it from proximity to the main heater and possible stray electric fields that may influence the flow measurements. The pipe through the flowmeter is reduced to $1\frac{1}{2}$ inches, schedule 40.

The primary pump is a two-stage electromagnetic conduction pump. The pumping section is fabricated from $1\frac{1}{2}$-inch schedule-10 pipe, which is flattened to produce a gap of approximately 1 inch between the inner pipe walls. Laminated nickel bus bars are nicrobrazed in a hydrogen atmosphere to the edges of the flattened pipe at each pumping stage. From the pump, the sodium flows through a U-bend of $2\frac{1}{2}$-inch pipe to the main heater.

The main heater consists of a 40-foot length of $1\frac{1}{4}$-inch pipe coiled as shown in figure 3 with one set of electric taps at each end and a third set in the center.

A 0.7-inch-diameter sharp-edge orifice maintains sufficient pressure upstream to prevent boiling within the main heater. The sodium flows through the orifice to enter a 10-foot length of 4-inch pipe where it is depressurized and flash vaporization occurs. The long run of 4-inch pipe provides thermal and dynamic equilibrium of the two-phase sodium mixture prior to entry into the separator.

Secondary system. - The sodium vapor that passes from the separator flows through a convergent nozzle into a vapor environmental chamber and then to an air-cooled condenser. The condensate enters an accumulator from which it flows through the secondary pump, flowmeter, and throttle valve before combining with the primary flow to complete the cycle.

The convergent nozzle has a throat diameter of 0.775 inch and is located in the 3-inch vapor piping at the entry to the vapor environmental chamber. The flow through the nozzle will be sonic when the pressure ratio across the nozzle is approximately one-half.

The environmental chamber is 12 inches in diameter and 18 inches long with the nozzle outlet located midway between the ends and perpendicular to the wall of the vessel (fig. 3). This vessel is provided for mounting erosion specimens or research vehicles to be tested within a vapor environment. The 3-inch pipe at the bottom of the chamber passes the vapors to the air-cooled condenser.

The condenser consists of eight U-shaped loops of 1-inch (O.D.) tubing with 2-inch-diameter fins that are connected to the horizontal 3-inch-pipe headers. A 1/2-inch pipe drains the condensate from the outlet header to the accumulator.

The accumulator is a vertical tank 12 inches in diameter and 30 inches long, which was sized to take up the increased volume of sodium due to thermal expansion. An added function of this vessel is to maintain a positive suction head on the secondary pump.

A 1/2-inch pipe from the bottom of the accumulator supplies the secondary pump, which pressurizes the sodium through the flowmeter and the throttling valve, and returns it to the primary system. The secondary pump and flowmeter are similar to those in the primary system, except that they are smaller in size and capacity. The throttling valve is a packless bellows-sealed valve that was installed to provide more uniform flow, and thus smoother control, and to suppress backflow from the primary system.

Oxide control and indicating system. - This system (OCI) is designed to remove sodium oxide from the system by both hot and cold traps and to measure the concentration of the sodium oxide by a plugging indicator (fig. 2). A 1/2-inch pipe joined to the primary-pump-outlet piping supplies sodium to the OCI system. A portion of this sodium is regulated by means of an 1/8-inch-diameter orifice through the hot trap. The remainder of the sodium flows through the outer annulus of a concentric tube economizer, a finned tube cooler, the cold trap or plugging indicator, the tube side of the economizer, and a flowmeter, and then recombines with the sodium from the hot trap before returning to the primary system at the inlet to the primary pump. The cold trap and plugging indicator are combined to utilize the same cooler and flowmeter.

The flow of sodium from the OCI cooler is controlled by packless bellows-sealed valves to either the cold trap (an 8-in.-diam. by 30-in.-long tank packed with stainless-steel wire mesh) or to the plugging indicator (a packless bellows-sealed valve with a serrated plug).

The hot trap is a 14-inch length of 3-inch pipe with a 6-inch column of titanium crystals. At temperatures in excess of 1200° F, the sodium oxide is chemically reduced as it flows through the bed of hot titanium.

Auxiliary systems. - A sump tank 2 feet in diameter and 5 feet long is provided to contain the sodium inventory when the system is not in operation and to drain the system if an emergency occurs during operation. The sump tank is connected to the process systems through a 1-inch pipe and valve at the liquid junction of the primary and the secondary systems (figs. 2 and 3). A 1/2-inch pressure-equalizing line and valve connects the top of the sump tank to the top of the accumulator.

A single-stage mechanical vacuum pump with a capacity of 130 cubic feet per minute is connected to the top of the sump tank through a dry ice and alcohol cold trap, a pneumatically operated shutoff valve, and a vapor trap. Evacuation of the sump tank and process systems from atmospheric pressure to 25 microns of mercury is accomplished in approximately 4 hours.

The inerting atmosphere is supplied to the system from a bank of argon cylinders through a pressure regulator, a high-pressure relief valve, a pneumatically operated shutoff valve, a vapor trap, and thence to the sump tank.

A sampling system (fig. 5) is located downstream of the pump outlet in both the primary and the secondary systems for the removal of liquid-sodium samples at operating temperatures. The systems consist of a sampling valve, a collector chamber, and a 10-cubic-centimeter sampling bucket. Radiant heaters preheat and maintain the sample temperature through the sampling valve and line to the collector chamber. With the sampling bucket turned aside, sodium flows into the collector to purge the system; then the sampling bucket is turned into position to receive the sample. Regulation of the collector-chamber pressure is provided through an inert gas and vacuum system. The excess sodium in the collector is drained through a valve located at the bottom of the chamber. After a sample has been taken and allowed to cool, it is removed by opening a flanged closure.

Electric Power System

The test cell is supplied with three-phase 2400-volt power feeders that serve two single-phase loads: (1) the main heater and (2) the auxiliary electric power system, which supplies the system trace heaters, the electromagnetic pumps, and the blower for the oxide control and indicating unit. A schematic drawing of the electric power system is included in figure 2.

Main heater. - The power system to the main heater is composed of (1) an oil-immersed contactor, (2) a saturable core reactor and magnetic amplifier, (3) a 240-kilovolt-ampere 2400/24-volt single-phase transformer, and (4) copper bus bars that interconnect the transformer and the stainless-steel bus bars, which are welded to the main heater.

The two halves of the 40-foot length of $1\frac{1}{2}$-inch pipe, which serve as the main heater, are connected as a parallel electric circuit. Twelve sections of 1/4-inch stainless-steel plate, 6 inches wide and 16 inches long with 1/4-inch spacing, are welded to the center of the heater. These bus plates are connected by copper bus bars to one of the transformer secondary taps. The top and bottom bus bars of the heater, each consisting of six sections of stainless-steel plate, are connected to the second transformer tap with copper bus bars. The parallel arrangement is used to minimize voltage potential across the ends of the heater to prevent current flow in other process piping. The bus bar arrangement is shown in figures 3 and 4(a).

The diameter and length of the main heater were sized to provide 180 kilovolt-amperes when 18 volts are impressed to the pipe heater.

Auxiliary electric power. - The auxiliary power system consists of (1) a single-phase two-pole 2400-volt load interrupter, (2) a 100-kilovolt-ampere 2400/480/240 volt single-phase transformer, and (3) a power distribution center.

The power distribution center includes appropriate breakers, relays, and contactors, which provide 480-volt power for the primary electromagnetic pump and 240-volt power for the secondary electromagnetic pump, the OCI blower, and the system preheaters.

Sheathed-resistance heaters provide 25 kilowatts of power for preheating the system prior to charging with sodium. The preheaters are energized by the manually operated switches.

The power circuits to the electromagnetic conduction pumps include variable autotransformers for regulating the voltage and capacitors for power-factor correction. The pump voltages are controlled by manually positioning the autotransformers.

Electric power for instruments, control systems, the condenser blower motor, and the vacuum pump is obtained from a separate power source.

Control

The desired process conditions are established and maintained by the control of three process variables: (1) the sodium outlet temperature of the main heater, (2) the vapor-condensation temperature, and (3) the flow rate in the primary circuit.

Main heater. - Power to the main heater is controlled by a three-mode temperature recorder-controller, which operates on an instream thermocouple located at the outlet of the heater. The output from the controller operates the saturable core reactor through a magnetic amplifier.

Condenser. - The temperature of condensation of the sodium vapors is controlled by a temperature recorder-controller, which operates on an instream thermocouple located in the bottom header of the condenser. The pneumatic output from the controller operates a damper in the outlet ducting of the condenser cooling air.

Primary pump. - The primary flow rate is controlled by positioning the autotransformer of the primary pump with a manual control unit that operates an electric-motor-drive assembly.

Instrumentation

Temperature. - Chromel-Alumel thermocouples are used to measure the temper-

atures of the system. Thermocouples used mainly for monitoring the system during preheating are surface mounted; those used for controlling and monitoring the process are located in instream wells.

The system temperatures of primary interest are monitored continuously and recorded on a multiple-point potentiometer-type instrument. Single-point continuous recorders are used to measure the vapor temperatures before and after the convergent nozzle. Temperatures of secondary interest are read from a single-point pyrometer equipped with selection switches.

The temperature of the sodium in the sump tank is maintained between the desired limits by an indicating galvanometer containing low- and high-limit meter relays, which provide on-off control to the tank heaters.

Pressure. - Process pressures are measured at three locations: (1) at the outlet of the main heater, (2) at the inlet to the convergent vapor nozzle, and (3) at the inlet to the air-cooled condenser. Null balance bellows-type transmitters equipped with regulating pilot valves to supply air to the transmitters are used. The process pressure is applied to the outside of the stainless-steel bellows, and transmitted air pressure is applied to the inside of the bellows to establish a balanced position.

The process pressures vary from 1 pound per square inch absolute to 20 pounds per square inch gage; the pressures at the nozzle inlet and the condenser inlet are always subatmospheric. To facilitate operation of the transmitter pilot-valve assemblies and the recording of system pressures, it is desirable that all transmitted pressures be above atmospheric pressure. This is accomplished by setting about a 15-pound-per-square-inch bias on the transmitter. Process pressures are recorded on a multipen instrument.

An inferential-type thermocouple gage is used to measure system pressures below 1000 microns of mercury. This gage is located in the evacuating line to the sump tank.

Liquid level. - The liquid levels in the separator and the accumulator are measured by radiation emitted from 25-millicurie sources of cesium 137. A beam of gamma radiation is directed through the vessel to Geiger tubes located diametrically opposite the radiation source. The radiation beam passing through the vessel produces an output current from the detector that is correlated with liquid level. The millivolt output signal from the detector circuit is recorded on a potentiometric-type instrument.

Flow. - The process system contains three magnetic flowmeters, equipped with permanent magnets, located in the primary, the secondary, and the OCI systems. The millivolt outputs from these meters, which are proportional to the flow rates, are recorded on strip-chart instruments.

Electric power. - Electric power to the main heater is monitored by a recording wattmeter, and indicating meters are used to measure the voltage and current applied to the main heater and both electromagnetic pumps.

Protective devices and alarms. - The system is equipped with devices that either give an audible and visual alarm or initiate a control action in the event of undesirable conditions in specific areas of the system. Pressure-actuated electric switches initiate the alarm system in the event of excessive transmitted pressures. Indicating galvanometers containing adjustable meter relays energize the alarm system in the event of high temperatures at the two electromagnetic pumps. A low-temperature meter relay energizes the alarm system if the sump-valve temperature drops to a value that would prevent emergency draining. A photoelectric device and a conductivity cell, incorporated in the condenser air outlet ducting, will also initiate the alarm system in the event of a sodium leak. In order to protect the main heater coil, an indicating galvanometer with a high-temperature meter relay and a low flow limit switch attached to the primary flow recorder are connected in series with the relay in the main-heater power supply. The power to the main heater is reset manually if either of the safety devices causes an interruption.

The control room is remotely located from the process system (fig. 6). Communication between the test cell and the control room is made by telephone. Observation of the test system is made through a window separating the two areas.

SYSTEM OPERATION

The process system, sump tank, OCI system, and sampling systems were preheated to 800° F and outgassed for 48 hours by continuous evacuation. The system was then pressurized with argon and allowed to cool to room temperature except for the sump tank, which was held at 350° F for charging with sodium. After 300 pounds of sodium were transferred into the sump tank, the system was in standby condition ready for operation.

Preheating and Evacuation

The system is preheated to 600° F, with the coolest areas at a minimum of 300° F prior to charging with sodium. The main heater is preheated at a rate of 2° to 4° F per minute by using the main heater power, while the remainder of the system is preheated by the line heaters. Power is applied to the secondary pump to aid in preheating; however, because of the higher voltage applied and the possibility of damaging the primary flow tube, the primary pump is energized only when filled with molten sodium. The time required to preheat the system to the preceding specified limits is approximately 4 hours. During the preheating operation, the system is evacuated to a pressure of 50 microns of mercury or less. The system leak rate at 25 to 50 microns pressure has proved to be less than 1 micron per hour.

Charging Sodium into Process System

The preheated and evacuated process system is isolated from the sump tank by closing the valve in the equalizing line and the sump valve. An argon gas pressure of 10 pounds per square inch absolute is established in the sump tank, and the sump valve is opened until the desired level is obtained in the separator.

The sump valve is closed and the sump tank, having a remaining inventory of 100 pounds of sodium, is evacuated to less than 500 microns.

Establishing Flow

A flow rate of 15 to 20 gallons per minute is established by slowly positioning the autotransformer with the electric-drive control unit, while observing the primary flow recorder. In order to provide sufficient inlet head to the primary pump, proper liquid level must be maintained in the separator. The level is maintained by intermittently pumping sodium from the accumulator to the primary system. The primary system is then heated to 800° F by increasing the main-heater-outlet temperature at a rate of 2° per minute. With the primary system at 800° F, flow is established through the OCI system and a plugging run is made to determine the concentration of sodium oxide in the sodium. A flow of approximately 1 gallon per minute is established through the cold trap to reduce the sodium oxide concentration. The primary system is operated at 800° F with continuous cold trapping until a plugging run indicates an oxide saturation temperature below 400° F.

Establishing Desired Process Conditions

With an oxide saturation temperature of 400° F or less, the desired primary flow rate is established, and the main-heater-outlet temperature is increased 2° per minute. Throughout the increase in temperature, the oxide saturation temperature is frequently determined, and cold trapping of oxides is made, if necessary. When the temperature of the primary system reaches 1200° F, the condenser air blower is used to circulate cooling air across the primary pump. The air is drawn from the test cell through an opening in the top of the enclosure to the pump. From the pump, the cooling air is ducted to the intake of the blower. If cooling air is not required for condensing, the air from the blower is discharged into the test cell.

The advance of the vapors from the separator to the condenser heats the process piping above the preheat temperature, at which time the line heaters are de-energized. When a temperature of 1000° F is attained in the condenser, the condenser temperature controller is activated. Air is supplied to the condenser either by natural convection or by a blower depending on the vapor-generation rate.

Until about 50 pounds per hour of condensate is produced, the secondary pump is used intermittently to maintain the liquid level in the separator. At higher vapor-generation rates and during steady-state operation the secondary pump is used continuously.

The pressure of the molten sodium at the outlet of the main heater is maintained at least 5 pounds per square inch above the vapor pressure to suppress boiling. Figure 7 shows the minimum permissible rates of flow and the corresponding pressures used to suppress boiling in relation to the main-heater-outlet temperature. This curve was determined experimentally.

Shutdown and Draining

The heater-outlet temperature is decreased 2° to 3° per minute to 1200° F, and the power to the main heater is turned off. During cooling of the primary circuit, the condenser temperature is decreased at that same rate to 1200° F. The condenser is sustained at 1200° F until the main heater temperature is 1400° F, at which time the condenser cooling air is discontinued. Below 1200° F, continued circulation of the sodium in the primary system provides a cooling rate of 1° to 3° per minute because of the small degree of flash vaporization and heat losses from the system. When a system temperature of 700° F is established, the primary and secondary pumps are de-energized, and the valves in the OCI system are opened. The system is drained by gravity by opening the sump valve and the equalizing line valve. The drained system is then pressurized with argon to 2 to 5 pounds per square inch gage.

OPERATIONAL PERFORMANCE

The system was operated for 800 hours during which time two 150-hour periods of uninterrupted operation at temperatures between 1300° and 1700° F were obtained. These periods of operation are shown in figure 8 to present the manner in which the heater-outlet and the condenser temperatures were varied and also to indicate the duration of settings. The resulting equilibrium temperature in the separator, which is also the temperature of the vapor entering the nozzle, is represented by the dashed lines. This temperature is affected by the primary circulation rate; wherever this rate is varied, the average temperature is plotted. The circulation rate was varied from 12,000 to 19,000 pounds per hour, and, over this range, the separator temperature varied 10° to 15° F.

At 394 hours of circulation, a temporary process upset was indicated by a rapid decrease in process temperatures (fig. 8(a)). Such process instabilities, general system characteristics, and process interruptions are discussed under PROCESS AND EQUIPMENT PROBLEMS.

At 664 hours of operation, with a heater-outlet temperature of 1600° F, the condenser temperature was increased from 1400° to 1500° F during which time the separator temperature increased (fig. 8(b)). This rise in separator temperature is indicative of a change from critical to restricted flow through the convergent vapor nozzle. A similar performance is noted at 699 hours of operation. These data are discussed in the section Nozzle Unchoking Data.

Data and Results

Steady-state data. - Typical steady-state data covering the full range of operating severities are listed in table I. Data for each run were recorded after steady operation had been sustained throughout the system for 2 to 10 hours. The heater-outlet temperature and the condenser-outlet temperature are measured at two locations; both sets of dual measurements show good agreement. Equally good agreement exists between the temperature of the saturated liquid in the separator and the equilibrium vapor entering the nozzle. The pressure trans-

mitters proved to be unreliable, and therefore pressure data are not tabulated.

A substantial temperature difference between the saturated liquid flowing from the condenser and the liquid in the accumulator is due to the long retention time in the accumulator and the consequent heat losses. The temperature of the expanded vapor is measured in the vapor environmental chamber and at the condenser inlet. Comparison of these temperatures with the condenser-outlet temperature indicates no substantial superheating. Data are shown for heater-outlet temperatures up to 1700° F, condensation temperatures up to 1495° F, and primary liquid-circulation rates as great as 18,800 pounds per hour. Measured rates of vapor generation are listed as secondary flow rates.

Electric power data are presented as kilowatts, amperes, and volts as measured at the secondary bus bars of the 240-kilovolt-ampere power transformer. The voltage drop across the top and bottom sections of the heater is also listed. The power factor for the system as determined by the data measured at the transformer varies from 0.77 at 57 kilowatts to 0.87 at 167 kilowatts.

Nozzle unchoking data. - The condition of maximum or critical flow in a nozzle is obtained when the ratio of velocity to specific volume is maximum. With the exhaust or receiving pressure of the nozzle equal to or less than the pressure needed to establish critical flow, the rate of flow for a fixed-area nozzle is independent of the receiving pressure and is determined by the temperature and pressure at the nozzle inlet. As the exhaust pressure is increased beyond the critical pressure, the flow decreases. Since this decrease in flow could not be observed readily directly in the system, temperature measurements had to be used as an indication of unchoking.

Table II shows nozzle data taken with a heater-outlet temperature of 1600° F and a primary flow rate of 18,800 pounds per hour. The temperature of the vapor entering the nozzle is taken as the average of the temperature of the saturated liquid in the separator and the temperature of the vapor at the nozzle inlet. The temperature of the saturated condensate is taken as the average of two measurements made at the bottom of the free-draining condenser. The condenser-inlet temperature is listed to show that no significant superheating is realized.

The data shown in table II were taken with the system initially at steady-state operation. The condenser temperature was increased incremently from 1396° to 1551° F and subsequently reduced stepwise to 1366° F. During the increase in condensing temperature (and pressure), the nozzle-inlet temperature increased, which indicates a change from critical to restricted flow through the nozzle. During reduction of the condensation temperature from 1551° to 1366° F, the nozzle-inlet temperature was reduced to a state at which a further decrease in condensing temperature (or pressure) had no effect on the upstream temperature; this indicated the transition from restricted to critical flow.

These data are shown as curve 2 in figure 9 as the variation of nozzle-inlet pressure p_3 with the ratio of condenser pressure to nozzle-inlet pressure p_6/p_3 for the corresponding temperatures listed in table II. These pressures were calculated from the vapor-pressure equation presented in reference 4:

$$\log p = 5.53103 - \frac{8718.30}{T - 83.2} \qquad (1)$$

The nozzle-inlet pressure is constant at a pressure ratio less than about 0.65. Further increase in condensing pressure, and consequently in pressure ratio, to 0.72 shows a 0.3-pound-per-square-inch increase in inlet pressure followed by a constant inlet pressure. Still further increase in condensing pressure provides another increase in inlet pressure.

The plateau in curve 2 at an inlet pressure of about 9.75 pounds per square inch apparently represents a shift in the thermodynamic path followed by the expanding vapors at or near a receiving pressure equal to the critical pressure. This may be indicative of a shift from a state of equilibrium during restricted or subcritical flow $p_6/p_3 > 0.80$ to supersaturated expansion for critical flow $p_6/p_3 < 0.65$.

Curves 1, 3, and 4 in figure 9 are additional nozzle unchoking data taken up to the initiation of restricted flow. The area left of the vertical dashed line represents critical flow through the nozzle; the area of restricted flow lies to the right.

Restricted flow is also well indicated by the decrease in electric power (table II) needed to sustain the heater-outlet temperature with constant primary flow rate during a rise in separator temperature.

These limited nozzle data, as tabulated in table II and presented in figure 9, indicate the presence of a change in the thermodynamic path of the expanding vapors (as indicated by a plateau) as the receiving pressure is increased up to and beyond the critical pressure. The nozzle data are based entirely on thermocouple measurements; and, although good agreement is noted between the two sets of dual temperature measurements, which were read on the same pyrometer, substantial error may be inherent in the data. The temperature data, however, should be interconsistent. Additional error is introduced by the use of the vapor-pressure equation. For example, curve 2 in figure 9 indicates an unusually high critical pressure ratio of 0.65. An error of $\pm 1/2$ percent in temperature measurement superimposed on an error of ± 3 percent in vapor-pressure data introduces a possible error of ± 15 percent in the critical pressure ratio.

It is apparent that proper investigation of the expansion process of alkali metal vapors under critical and restricted-flow conditions must be made directly by obtaining reliable and accurate pressure measurements in a nozzle. Such data with proper analysis will give valuable insight into the effect of the dimerization reaction, supersaturation, and unusual general properties of the metallic vapors in the expansion process.

Experimental critical vapor flow rates. - From the steady-state data in table I and the enthalpy data from reference 4, the vapors generated by the flashing process were calculated to compare with the measured secondary flow rates. The quality x, or fraction vaporized, of the two-phase mixture after flashing is determined from

$$x_2 = \frac{h_1 - h_{f,2}}{h_{g,2} - h_{f,2}} \tag{2}$$

which is used to calculate the vapor-generation or secondary flow rate from

$$w_s = x_2 w_p \tag{3}$$

The enthalpy of the liquid at the heater outlet is based on the average of the two heater-outlet temperatures. The average of the separator and nozzle-inlet temperatures was used to determine the enthalpy of the saturated phases after flashing. The calculated secondary flow rates are listed in table III. Use of equation (1) to find the nozzle-pressure ratio p_6/p_3 for these flow rates and comparison with the data in figure 9 indicate that the flow rates in runs 10, 11, and 15 were subcritical. The data for these three runs were omitted from the critical flow data plotted in figure 10. The data are fitted with the curve,

$$\frac{w_s}{A_t} = 51.46 + 43.75\ p \tag{4}$$

where the lowest nozzle-inlet pressure is 2.5 pounds per square inch absolute.

The measured flow rates are also listed in table III and plotted in figure 10. A comparison of the two curves shows a marked difference. The curve for the flows calculated by equation (3) is linear but fails to intersect the origin when extrapolated. Instead, at zero pressure, a flow rate of 51.46 pounds per hour per square inch is indicated; this is attributed to substantial error in temperature and primary flow measurements. In addition, some error may be introduced by the enthalpy values, particularly those for saturated vapor, which depend on the degree of chemical association.

The curve for measured flow is parabolic with a possible intercept at the origin. Flow rates less than 300 pounds per hour per square inch show a possible linear correlation parallel to curve 1 and properly indicate no flow at zero pressure. At higher flow rates, the marked deviation from linearity is attributed to flowmeter inaccuracy and errors inherent in the method of measuring the secondary flow at the outlet of the accumulator. The flows were taken from a theoretically calculated calibration curve. The flow rates were determined by adjusting the secondary pump to sustain a constant level in the accumulator for a reasonable period of time noting the constant millivolt signal from the magnetic flowmeter.

Theoretically Calculated Critical Vapor Flow Rates

For further evaluation of the results found for vapor flow from the steady-state data, theoretical calculations were carried out for flow in the nozzle. Two possible types of flow were considered: (1) equilibrium expansion and (2) supersaturated expansion. Other types are possible, but the two chosen would

probably provide the boundaries of flow predictable by existing thermodynamic data for sodium vapor. Thermodynamic data from reference 4 were used except where noted otherwise. The calculations for both situations are for an isentropic process, and the vapor phase is assumed to behave as a perfect gas. It is also assumed that the vapor flowing into the nozzle is saturated.

Equilibrium expansion. - During an equilibrium expansion of a vapor below the saturated state, condensation progresses continuously and phase equilibrium exists throughout the expansion process. Also, it is assumed that chemical equilibrium of the vapor-phase reaction of monatomic and diatomic sodium exists.

The critical mass-flow rate at various inlet pressures was determined by calculating V_x/v_x from the continuity equation

$$\frac{w_s}{A_x} = \frac{V_x}{v_x} 25 \tag{5}$$

and plotting these values against p_x/p_o to determine the maximum (critical) value of w_s/A_t.

The velocity of the expanding vapor, with inlet velocity neglected, was calculated from the equation

$$V = 223.8 \sqrt{h_o - h_x} \tag{6}$$

The enthalpy at state x was determined from

$$h_x = x_x h_{g,x} + (1 - x_x) h_{f,x} \tag{7}$$

where the quality, since the process is isentropic, was determined from

$$s_o = s_x = x_x s_{g,x} + (1 - x_x) s_{f,x} \tag{8}$$

The specific volume was calculated from

$$v_x = x_x v_{g,x} + (1 - x_x) v_{f,x} \tag{9}$$

The calculated results of critical mass flow w_s/A_t as a function of nozzle-inlet pressure are included in figure 10. The data fall along a straight line described by the equation

$$\frac{w_s}{A_t} = 38.75\ p_o \tag{10}$$

Supersaturated expansion. - Actual condensation during expansion may be delayed and cause the sodium vapor to be in a metastable or supersaturated state. In this state, the vapor is more dense than when it is in equilibrium at the same pressure. Expansion in this state results in a lower velocity; however, the

fractional increase in density is greater than the decrease in velocity and a greater rate of flow results than for an equilibrium expansion. It is assumed that supersaturation continues beyond the throat of the nozzle.

Where supersaturation is concerned, it is assumed further that the expansion proceeds too rapidly to allow any change in the chemical association of the vapor species and that throughout the expansion process the molecular weight of the vapor is unchanged from the initial-state point.

Treating the process in the nozzle as isentropic (with no condensation assumed) and the sodium vapor as a perfect gas permits calculation of the critical pressure and temperature directly by the following equations, with inlet velocity neglected:

$$p_c = p_o\left(\frac{2}{\gamma + 1}\right)^{\gamma/\gamma-1} \tag{11}$$

$$T_c = T_o\left(\frac{2}{\gamma + 1}\right) \tag{12}$$

where γ for the vapor-species mixture is calculated from the specific-heat data for monatomic and diatomic sodium vapor from reference 5 by

$$C_{p,m} = X_{Na_1} C_{p,Na_1} + \left(1 - X_{Na_1}\right) C_{p,Na_2} \tag{13}$$

$$C_{v,m} = C_{p,m} - \frac{R}{J} \tag{14}$$

$$\gamma = \frac{C_{p,m}}{C_{v,m}} \tag{15}$$

The critical velocity is then directly calculated from equation (6) where now

$$h_o - h_c = \frac{C_{p,m}}{M_m}\left(T_o - T_c\right) \tag{16}$$

and the specific volume is calculated from

$$V_{g,c} = \frac{RT_c}{p_c M_m\ 144} \tag{17}$$

The critical mass-flow rates w_s/A_t calculated in this manner are included in figure 10. The data fall along the line approximated by

$$\frac{w_s}{A_t} = 42.3\ p_o$$

A comparison of the two theoretical curves in figure 10 shows that the supersaturated expansion provides a significantly larger flow (~10 percent) than equilibrium expansion, but still does not substantiate the wide deviations of curves 1 and 4. It is noted, however, that reasonable agreement exists between the slopes of curves 1 and 2, and that curve 2 (supersaturated expansion) is a reasonable correlation for the measured data, curve 4, at low values.

PROCESS AND EQUIPMENT PROBLEMS

During the period of operation of the two-phase flash-vaporization facility in this investigation, process instabilities were encountered as a result of the loss of heater power, rapid changes in primary flow, or the leakage of air into the system.

Equipment problems encountered during this period were: (1) the failure of valve bellows, welds, and two electromagnetic conduction pumps, (2) the inability to obtain liquid-metal samples at operating conditions, and (3) the unreliable performance of process pressure and liquid-level instrumentation.

Process Instabilities

Interruptions in the main heater power were caused by improper functioning of protective devices. At 394 hours of operation, an abrupt decrease in heater-outlet temperature occurred from 1675° F with a separator temperature of 1590° F and critical vapor flow provided by a condenser temperature of 1350° F (fig. 8(a)). With the cessation of heater power and a primary flow of 50 gallons per minute, the heater cools rapidly to the separator temperature, and the vapor-generation rate is quickly reduced. The flow of vapors from the separator into the condenser reduces the pressure in the separator, which in turn induces flashing of the liquid in the separator. The subsequent momentary increase in separator pressure suppresses flashing until the flow into the condenser again lowers the separator pressure. During this repeated cyclic flashing, the inlet head to the primary pump is greatly varied; the primary flow oscillated from 5 to 50 gallons per minute, which prevented resetting the heater power. Stable operation was reestablished after 3 to 5 minutes, at which time the temperature in the primary circuit was 1350° F, and the condenser temperature had decreased to about 800° F. This process upset, caused by loss of heater power, was less drastic at lower temperatures where there was less variation of vapor pressure with temperature.

The liquid level of the sodium is maintained within prescribed limits in the separator to provide sufficient suction head for the primary pump. Increasing the primary flow rate reduces the liquid inventory in the separator plenum; the sodium is apparently contained in the conical section of the separator as a vortex. This vortex is frequently disrupted, as indicated by rapid increases in the liquid level in the separator plenum. Dumping of the vortex occurs infrequently

during normal operation of the system; however, too rapid a change in the primary circulation rate, surging of the primary pump, or vibration of the process piping due to gases in the primary circuit cause frequent dumping.

Minimum permissible flow at heater-outlet temperatures greater than 1550° F (fig. 7) provides a pressure above atmospheric between the primary pump and the sharp-edged orifice. With this exception the remainder of the system is operated at subatmospheric pressures; consequently, a leak in the process components may introduce air into the system. The failures that occurred were in the liquid-phase components of the system and, with one exception, the gas so introduced passed through the primary pump. The circulation of gas in the primary circuit is indicated initially by pronounced vibration throughout the system accompanied by noises of varying intensities, especially downstream of the primary pump. These cavitation-type noises are also reflected by a widely oscillating heater-outlet pressure and a slightly oscillatory primary flow rate. Generally, operation under these conditions has to be continued until the leak is located. In a few instances, the migration of nitrogen to the condenser has made the condenser completely ineffective. The noncondensable gas causes the pressure in the condenser to approach the pressure in the separator. As the condenser and separator pressures converge, the flow of vapors from the separator ceases, and the separator temperature rises to suppress completely the flashing process.

Throttling of the valve at the outlet of the secondary pump proved to be unnecessary to maintain stability between the primary and the secondary circuits.

Equipment Problems

Valves. - Three failures of multiply seamed bellows-sealed valves located in the oxide control and indicating system interrupted operation because of air leakage into the system. The valves failed at the welded seam of the bellows and at the weld joining the bellows to the upper sealing ring. These failures occurred after 10 to 100 cycles and in less than 100 hours of operation. The normal service temperature of these valves was 300° to 800° F with limited use at 1000° F.

The 1/2-inch OCI system valves and the 1-inch sump valve leaked internally across the seat throughout the operation. The leakage through the sump valve necessitated the frequent addition of sodium to the process during operation.

Pipe-weld failures. - Two pipe-weld failures occurred during the 800 hours of operation. The locations of these failures were at (1) the junction of the pressure transmitter to the heater outlet and (2) the junction of the separator effluent and the condensate return.

The weld joining the 1/2-inch pipe from the pressure transmitter to the heater outlet failed at the $1\frac{1}{4}$- by $\frac{1}{2}$-inch reducing tee after 240 hours of operation. The stress failure was caused by the expansion of the 10-foot length of 4-inch pipe from the anchored separator toward the main heater. Expansion of this flash line is allowed for by an expansion loop at the top of the heater; however, the pressure transmitter was unable to move with the expanding pipe be-

cause it was forced against the insulation of the stationary heater, thus the stresses that resulted in failure were induced. Figure 11 shows the external and internal views of the failure. Figure 11(a) shows the corrosive effect of sodium at high temperatures in an air atmosphere. The presence of the leak was indicated initially during operation at subatmospheric pressure by noises emanating from the primary circuit due to air entering the system. As the heater-outlet temperature was increased, the resulting outlet pressure exceeded atmospheric pressure and sodium began to leak out, as evidenced by smoke filling the test cell, which terminated the operation until repairs were made.

A weld failure occurred at the junction of the separator liquid effluent line and the condensate return line. Figure 12 shows the $2\frac{1}{2}$-inch tee junction with eccentric reducer. Liquid from the separator enters downward into the tee joining the condensate entering through the $2\frac{1}{2}$- by 1-inch eccentric reducer, and the combined streams flow to the left through a $2\frac{1}{2}$-inch pipe to the flowmeter and the pump. The failure occurred along the boundary of the weld joining the reducer to the tee and extended into the weld as shown in figure 13. Figure 12 also shows the location at the bottom of the tee where the junction was welded to an A-frame anchored to the bedplate.

The failure occurred after 700 hours of circulation in the primary circuit. The following table summarizes the service history of the failed area:

Cumulative time, hr	Separator effluent temperature, ^{o}F	Condensate temperature, ^{o}F	Remarks
170	<1000	---------	Negligible vapor generation; secondary pump line maintained at 300° to 500° F with line heaters
180	1000-1300	600-1000	Low vapor-generation rate; secondary pump used intermittently
165	1300-1500	1000-1400	Secondary pump used continuously
215	1500-1600	1350-1450	Secondary pump used continuously

With a separator temperature less than 1200° to 1300° F, the vapor-generation rate is not sufficient to require continuous use of the secondary pump; whereas, with a separator temperature above 1300° F, the secondary pump is used continuously. A temperature difference of 150° to 300° F between the separator effluent and condensate streams occurred with separator temperatures above 1300° F; however, with a separator temperature less than 1300° F, greater differences in temperature may exist; therefore greater thermal stresses at and near the junction of the streams are introduced.

Metallographic examination of the failed area indicated a stress-corrosion failure that was hastened by circumferential grinding marks on the inside wall of the assembly. The grinding marks were quite apparent in the weld as well as in the adjacent areas of the tee reducer, which indicates that the fabricator used a grinder to clean the welded area.

The cycles of heating and cooling in the failed area were severe enough to produce spheroidizing of the carbides as shown in figures 14 and 15, at the inside surface near the failure. The carbide formation in the reducer section (fig. 14) is much more excessive than in the tee (fig. 15). A chemical analysis of the two sections indicates that the difference in spheroidizing was not due to

Constituent	Weight, percent	
	Reducer	Tee
Carbon	0.06	0.06
Silicon	.40	.30
Molybdenum	2.59	2.6
Nickel	13.1	13.7
Chromium	17.9	16.8

chemical-composition variables but more likely is the result of prior metallurgical history. Such carbide formation depletes the material of alloying constituents, reduces its strength, and makes it notch and corrosion sensitive. Figure 14 includes one of many stress-corrosion cracks progressing from the root of a grinding mark and also shows overall severe straining not found in figure 15.

The condition of the material at the inside surface 3 to 4 inches away from the failure area is shown in figures 16 and 17. The structure of the tee section (fig. 17) is normal for type 316 stainless steel. Heavy strain is again shown in the reducer section (fig. 16). Although these grain boundaries are carbide laden, no spheroidizing is shown. This condition indicates that the entire reducer section was under stress and that there were excess carbides in the reducer section originally.

Figure 18 shows a crack in the root pass of the weld. Because carbides were larger and heavily concentrated in the grain boundaries, crack propagation in this area was primarily intergranular and confined to the root pass. This indicates a limited life expectancy for these areas and is not a cause for failure.

With separator-effluent temperatures less than 1300° F, the secondary pump was used periodically to transfer sodium from the accumulator to the primary system. The temperature of the condensate was as low as 600° to 800° F; thus, thermal cycling at the junction was introduced. It is concluded that the thermal cycling, the scoured condition of the failed area, and the fact that the tee was a fixed member and would serve as a concentration point for general piping stresses were the principal causes of the failure.

Electromagnetic-pump failures. - Two two-stage electromagnetic conduction pumps located in the primary circuit failed in a similar manner. The first pump (pump A) contained a flattened pumping section with a 0.6-inch gap between the inner pipe walls. The second or replacement primary pump (pump B) had a pumping section with a 1-inch gap to conserve static inlet head. Both pumps were designed to provide a 25-pound-per-square-inch pressure increase at a flow of 50 gallons per minute of saturated liquid sodium from the separator at 1350° to 1620° F with an inlet head of 4 feet of sodium.

Pump A failed after 110 hours of operation of which 45 hours were with sodium at temperatures above 1200° F including 5 hours of operation at 1575° F followed by the failure. The pump cavitated and surged throughout the 110-hour operation. The cavitating and chugging noises were emitted from the bottom section of the heater as well as from the pump. At temperatures below 1300° F, flow rates greater than 20 gallons per minute caused noise of such intensity accompanied by pronounced vibration of the process assembly that higher flow rates were judged unsafe. A maximum flow of 42 gallons per minute was attained at temperatures above 1400° F. Cavitation was slight above 1400° F; however, surging was present at all conditions of flow.

Pump A failed at the outlet of the first pumping stage. Figure 19(a) shows the pumping section with the nickel bus bars attached; flow is from left to right. Figure 19(b) is a closer view of the inlet stage with the top hole indicated by the pencil point at the right end of a 1-inch-long crack along the margin of the braze. Opposite the top hole a second hole (not shown) about 1/16 inch in diameter was located. It appeared that the failure originated on the top side of the flow tube, where air entered the pipe, impinged and burned through the opposite wall, and formed the bottom hole.

Metallurgical examination of the failure showed that the crack progressed transgranularly. There was no evidence of intergranular oxide inclusions or fissures through the grain boundaries. The crack was apparently formed by repeated cyclic stressing at the edge of the brazed joint. The brazed joint between the bus bar and the pipe was very poor quality, since the inner 50 percent of the joint contained no brazing material. Such inferior brazing results in localized hot spots due to high current densities. The perimeter of the brazed joint was well fitted and of good quality, but apparently the fit between the curved edge of the flattened flow tube and the bus bar was not properly maintained during the brazing operation.

The gap at each pumping stage of the flow tube was reduced during operation from 0.6 inch to 0.3 to 0.4 inch. This occurred only at the pumping stages where the field coils and transformer iron were placed against the flow tube. This reduction in flow area would promote cavitation. Little cavitation damage was noted in the first pumping stage; however, pronounced pitting of the second stage was apparent.

The natural vibration of the pump assembly induces flexure at the joint of the massive nickel bus bars and the thin-walled flow tube. This vibration also provided impetus for eventual compression of the tube between the field coils. This compression introduces additional stresses at the braze margin. A hot spot

caused by (1) the interaction of the magnetic flux and the bus bar current and (2) a high current density caused by a poorly brazed joint, along with the stresses, apparently induced the failure.

Pump B, equipped with larger field coils, was supplied with a 1-inch gap and, although constructed with better brazing techniques, failed after 700 hours of operation. Sodium at temperatures from 1450° to 1600° F was circulated for 325 hours prior to the failure of the flow tube. The pump gave no indications of surging or cavitation during the operation. All noises from the pump could be attributed to gas in the system introduced by air leaking into the system.

Pump B failed just inside the inlet of the second stage in a manner similar to the failure described previously. The top section in figure 20 is an inside view of the tube and shows a crack about 1 inch long extending along the braze boundary with the small single hole appearing as a light-colored area. Both sections of the flow tube show pitting caused by electrical hot spots and apparently some cavitation damage. This figure also shows that the original gap of 1 inch was reduced to 3/4 inch where the field coils were mated to the pumping section. The brazed connection was of good quality; about 95 percent of the contact area between the bus bar and the flow tube was firmly attached, as indicated by radiography. The failure of this flow tube was apparently due to the stresses induced by the weight of the poorly supported transformer iron and localized electric heating at the inlet of the second stage caused by the interaction of the magnetic field and the bus bar current.

Liquid-metal sampling. - Several unsuccessful attempts were made to obtain a liquid-metal sample during operation of the system. Improper pressure regulation of the sampling system resulted in either flooding the process system with argon or flooding the sampling system, including argon and vacuum lines, with sodium.

Instrumentation. - Two principal instrumentation problems encountered were the unreliable operation of the pressure transmitters and the erratic operation of the liquid-level devices.

As mentioned in the section on controls and instrumentation, null balance bellows-type pressure transmitters, biased to transmit positive pressures, are used at three locations in the process system. Calibrations of the pressure transmitters are made prior to system startup, and recalibrations are made periodically during the period of operation. These transmitters have proved to be unreliable because of the continual drifting of the calibration; however, this is a zero shift only, and there is no apparent change in the sensitivity of the transmitter. For a fixed system pressure, the transmitted pressure decreased with time, as shown in figure 21. Because of the bias, the bellows is under tension and moves away from the nozzle, thus transmitting increasingly lower pressures with continued use. Rebiasing was required on two of the transmitters after a decrease of 3 to 4 pounds per square inch in transmitted pressure.

The performance of the liquid-level devices was erratic and considered marginal. The intensity of the random radiation received by the detector varied greatly with a fixed level in the vessel. Because of the low radiation intensity of the source used and considerable background effects, an optimum time constant

of 30 seconds for the setup resulted in sluggish measurements. The measuring instruments also indicated 3 to 5 percent of full-scale (10 mv) cyclic variation. Initially, the secondary pump was installed to be controlled automatically from the liquid level in the separator. With the sluggish response and the cyclic variations resulting in essentially on-off operation, the pump was disconnected from the liquid-level device and controlled manually.

Modifications to System

The structural repairs and modifications to the system are as follows:

(1) The valve-bellows failures are attributed to the low quality of the bellows and to the fact that the design of the valve was not compatible with its intended service in the system. The OCI system valves have been replaced by a different type, modified to NASA specifications, with a seamless bellows that has a large number of convolutions to minimize the stress effects. These valves will also exhibit better throttling and seating characteristics.

(2) The failure of the weld joining the pressure transmitter to the heater-outlet piping was a result of an oversight of the fabricator. Reoccurrence of this failure was eliminated by removing sufficient insulation from the stationary heater pipe to allow unobstructed movement of the repaired transmitter and piping.

(3) Thermal stresses, induced by the relatively cold condensate return and the separator effluent, were partly the cause of the failure at the junction of the two streams. In order to minimize the thermal stresses in this area, a concentric tube was extended from the 1/2-inch-pipe condensate-return line through the $2\frac{1}{2}$-inch-pipe tee and eccentric reducer. This concentric tube allows the colder liquid sodium to be heated by the separator effluent prior to their mixing at a location approximately 2 inches downstream of the outlet of the $2\frac{1}{2}$-inch tee.

(4) At the severe operating conditions of the primary pump, the flattened flow tube is very susceptible to stress failures at the pumping sections. A replacement pump will be equipped with a modified flow tube, which has elliptical cross section and which will be less susceptible to fatigue failure. Additional support will be provided for the transformer iron and bus bars to prevent external stress and compression of the pumping sections.

(5) The sampling devices supplied with the system proved to be totally unsatisfactory and will be replaced by a sampling bypass around each pump. Valves, with proven capabilities to 1600° F, will be incorporated in the sampling systems and will allow the liquid sodium to be sampled at stream temperatures.

CONCLUSIONS

The initial operation of the sodium flash-vaporization system has proved the general feasibility and versatility of the process scheme. The system is valu-

able in introducing personnel to liquid-metal technology and to the operation of integrated process systems. The specific conclusions pertaining to the process scheme after 800 hours of operation are as follows:

1. Stable system operation is attainable throughout the range of design parameters. No process instabilities occurred during the flashing process during either transient or steady-state operation.

2. No changes in basic design of the system are needed to achieve the project objectives.

3. The initial operation of the system is considered to be a qualitative general performance run, and the data presented herein are indicative of the capabilities of the system. The vapor mass rates of flow through the convergent nozzle as determined by heat balances differ greatly from direct measurements of the condensate. The errors inherent in both methods of determining critical flow data preclude definite conclusions; however, the data indicate that critical flow rate is best approximated by a supersaturated expansion with the assumption that the vapors behave as an ideal gas.

4. Errors in research data and process-control difficulties introduced by deficient pressure, flow, and liquid-level devices have been defined and serve as a basis for a separate program to evaluate and develop instrumentation components having the stability and accuracy needed for high-temperature two-phase alkali-metal systems.

Lewis Research Center
National Aeronautics and Space Administration
Cleveland, Ohio, January 7, 1963

REFERENCES

1. English, Robert E., Slone, Henry O., Bernatowicz, Daniel T., Davison, Elmer H., and Lieblein, Seymour: A 20,000-Kilowatt Nuclear Turboelectric Power Supply for Manned Space Vehicles. NASA MEMO 2-20-59E, 1959.

2. Moffitt, Thomas P., and Klag, Frederick W.: Analytical Investigation of Cycle Characteristics for Advanced Turboelectric Space Power Systems. NASA TN D-472, 1960.

3. Lieblein, Seymour: Analysis of Temperature Distribution and Radiant Heat Transfer Along a Rectangular Fin of Constant Thickness. NASA TN D-196, 1959.

4. Sittig, Marshall: Sodium - Its Manufacture, Properties and Uses. Reinhold Pub. Corp., 1956.

5. Evans, William H., Jacobson, Rosemary, Munson, Thomas R., and Wagman, Donald D.: Thermodynamic Properties of the Alkali Metals. Jour. Res. Nat. Bur. Standards, vol. 55, no. 2, Aug. 1955, pp. 83-96.

TABLE I. - STEADY-STATE DATA

Run	Temperature, °F										Measured flow rate, lb/hr		Electric power at main heater				Power factor
	Heater outlet (state 1)		Separator (state 2)	Nozzle inlet (state 3)	Vapor environmental chamber (state 5)	Condenser inlet (state 5)	Condenser outlet (state 6)		Accumulator (state 6')	Heater inlet (state 9)	Primary system, w_p	Secondary system, w_s	kw	amp	Volts		
	Location 1	Location 2					Location 1	Location 2							Transformer	Heater circuit	
													(a)	(a)		Top Bottom	
1	1350	1357	1321	1321	1200	1200	1194	1197	1109	1314	12,810	60	57	6,800	10.9	8.8 9.9	0.77
2	1400	1405	1365	1365	1208	1203	1197	1200	1112	1356	12,770	60	67	7,400	11.9	10.1 10.8	.76
3	1400	1406	1374	1373	1260	1256	1250	1251	1215	1367	18,110	68	67	7,400	11.8	10.0 10.6	.77
4	1500	1505	1456	1455	1353	1352	1353	1355	1325	1449	18,280	115	93	8,400	13.7	11.0 12.5	.81
5	1500	1505	1444	1442	1351	1357	1351	1354	1267	1427	12,410	108	94	8,450	13.7	11.7 12.4	.81
6	1550	1553	1493	1492	1349	1352	1349	1350	1322	1485	16,470	151	108	8,950	14.7	12.8 13.7	.82
7	1550	1555	1484	1483	1349	1353	1349	1351	1292	1472	12,900	139	107	8,900	14.8	12.8 13.7	.81
8	1550	1557	1495	1495	1349	1354	1350	1351	1332	1489	16,090	164	108	8,950	14.8	12.8 13.7	.81
9	1550	1554	1498	1498	1395	1400	1396	1400	1367	1495	18,790	164	107	8,900	14.7	12.8 13.6	.82
10	1550	1554	1494	1493	1428	1435	1432	1433	1410	1485	15,690	138	105	8,870	14.5	12.5 13.4	.83
11	1600	1602	1532	1532	1490	1495	1495	1495	1450	1520	14,270	155	114	9,000	15.1	13.3 14.0	.84
12	1600	1604	1538	1538	1395	1400	1395	1397	1374	1531	18,800	243	127	9,550	15.8	14.0 15.0	.84
13	1625	1627	1547	1546	1351	1355	1350	1353	1323	1537	15,590	253	137	9,840	16.3	14.6 15.4	.86
14	1650	1654	1561	1561	1347	1347	1342	1347	1321	1549	15,070	289	148	10,120	16.9	15.2 16.0	.86
15	1650	1655	1564	1564	1479	1484	1481	1484	1448	1554	14,210	212	143	9,850	16.6	15.0 15.7	.88
16	1650	1650	1568	1568	1395	1398	1394	1397	1375	1560	16,050	298	145	10,050	16.8	15.2 15.9	.86
17	1650	1650	1565	1564	1350	1350	1346	1349	1322	1552	15,870	288	150	10,180	17.0	15.2 16.1	.87
18	1650	1652	1576	1575	1352	1350	1347	1350	1325	1567	18,680	337	149	10,200	17.0	15.3 16.1	.86
19	1700	1700	1601	1601	1395	1400	1395	1396	1377	1585	16,080	341	167	10,600	18.2	16.3 17.2	.87

[a]Measured at transformer.

TABLE II. - NOZZLE UNCHOKING DATA

[Main-heater-outlet temperature, 1600° F; primary flow rate, 18,800 lb/hr.]

Time, min	Temperature, °F					Electric data at transformer bus bar			
	Separator (state 2)	Nozzle inlet (state 3)	Condenser inlet (state 5)	Condenser outlet		volts	amp	kva	kw
				Location 1	Location 2				
0	1538	1538	1400	1395	1397	15.8	9550	150.9	127
19	1536	1535	1409	1405	1410	15.8	9500	150.1	126
72	1540	1539	1423	1420	1424	15.8	9500	150.1	127
85	1539	1538	1433	1427	1425	15.8	9500	150.1	125
145	1542	1542	1475	1473	1476	15.8	9450	149.3	125
155	1545	1545	1490	1485	1489	15.6	9300	145.1	123
163	1545	1545	1497	1492	1495	15.4	9100	140.1	118
172	1546	1546	1511	1507	1510	15.3	9050	138.5	116
180	1555	1555	1530	1525	1528	14.9	8800	131.1	108
197	1560	1562	1553	1550	1552	13.8	8050	111.1	92
232	1560	1560	1553	1550	1552	13.6	8000	108.8	90
250	1560	1560	1552	1548	1550	13.5	7900	106.7	88
260	1555	1555	1546	1542	1546	13.8	8050	111.1	91
280	1549	1549	1526	1523	1525	14.8	8700	128.8	106
292	1545	1545	1515	1511	1516	15.0	8900	133.5	110
308	1544	1544	1510	1506	1509	15.1	9000	135.9	114
325	1540	1540	1500	1497	1500	15.2	9200	139.8	117
335	1540	1540	1490	1485	1490	15.3	9200	140.8	117
345	1540	1539	1480	1476	1480	15.4	9225	142.1	120
355	1536	1536	1473	1468	1471	15.7	9400	147.6	123
367	1537	1536	1460	1456	1460	15.6	9350	145.9	123
375	1535	1535	1447	1444	1446	15.7	9400	147.6	124
385	1536	1536	1434	1430	1435	15.7	9400	147.6	125
395	1537	1535	1422	1418	1422	15.7	9500	149.2	128
415	1538	1537	1403	1399	1398	15.7	9450	148.4	126
430	1535	1535	1370	1365	1367	15.7	9550	149.9	128

TABLE III. - VAPOR-GENERATION RATES

Run	Fraction of primary liquid vaporized, x_2	Vapor rate, w_s/A_t, lb/(hr)(sq in.)		Nozzle-inlet pressure, p_3, lb/sq in. abs	Pressure ratio, p_6/p_3
		Calculated from enthalpy balance	Measured		
1	0.0059	162	129	2.49	0.40
2	.0067	184	129	3.36	.30
3	.0055	212	145	3.57	.42
4	.0087	338	244	5.95	.52
5	.0109	287	229	5.51	.56
6	.0111	389	318	7.39	.41
7	.0125	343	296	7.02	.43
8	.0108	370	351	7.48	.41
9	.0101	402	350	7.61	.55
10	.0110	368	293	7.44	.70
11	.0129	390	331	9.51	.79
12	.0119	478	516	10.61	.39
13	.0149	493	537	9.99	.31
14	.0170	544	618	10.78	.27
15	.0166	504	452	10.95	.64
16	.0153	522	635	11.19	.37
17	.0160	539	611	11.01	.27
18	.0142	566	720	11.67	.26
19	.0189	644	730	13.29	.31

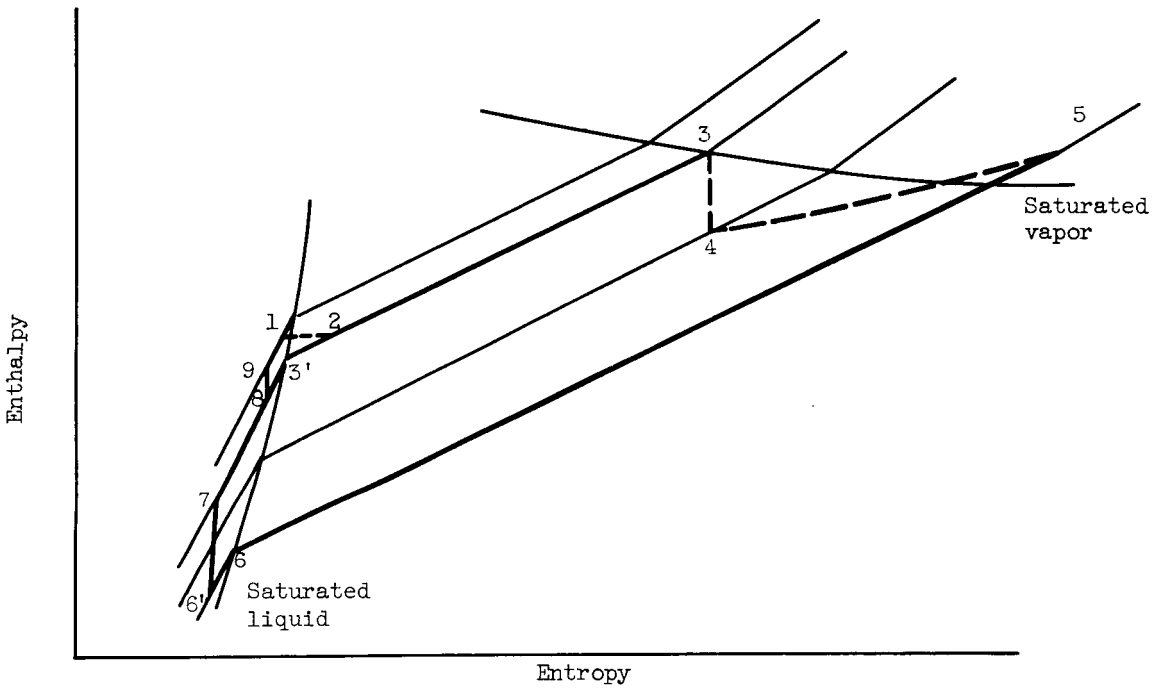

(a) Enthalpy-entropy diagram.

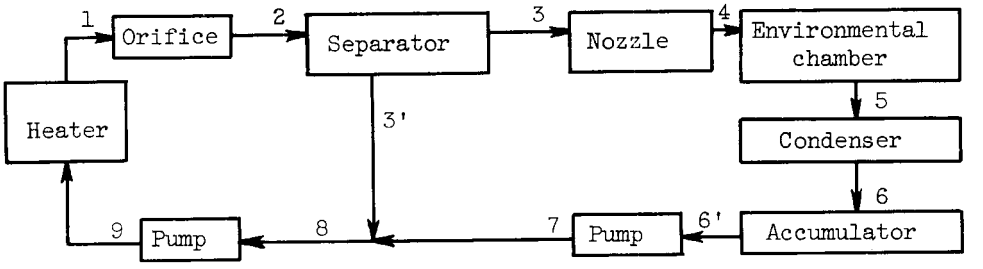

(b) Schematic diagram of system.

Figure 1. - Thermodynamic cycle of sodium flash-vaporization facility.

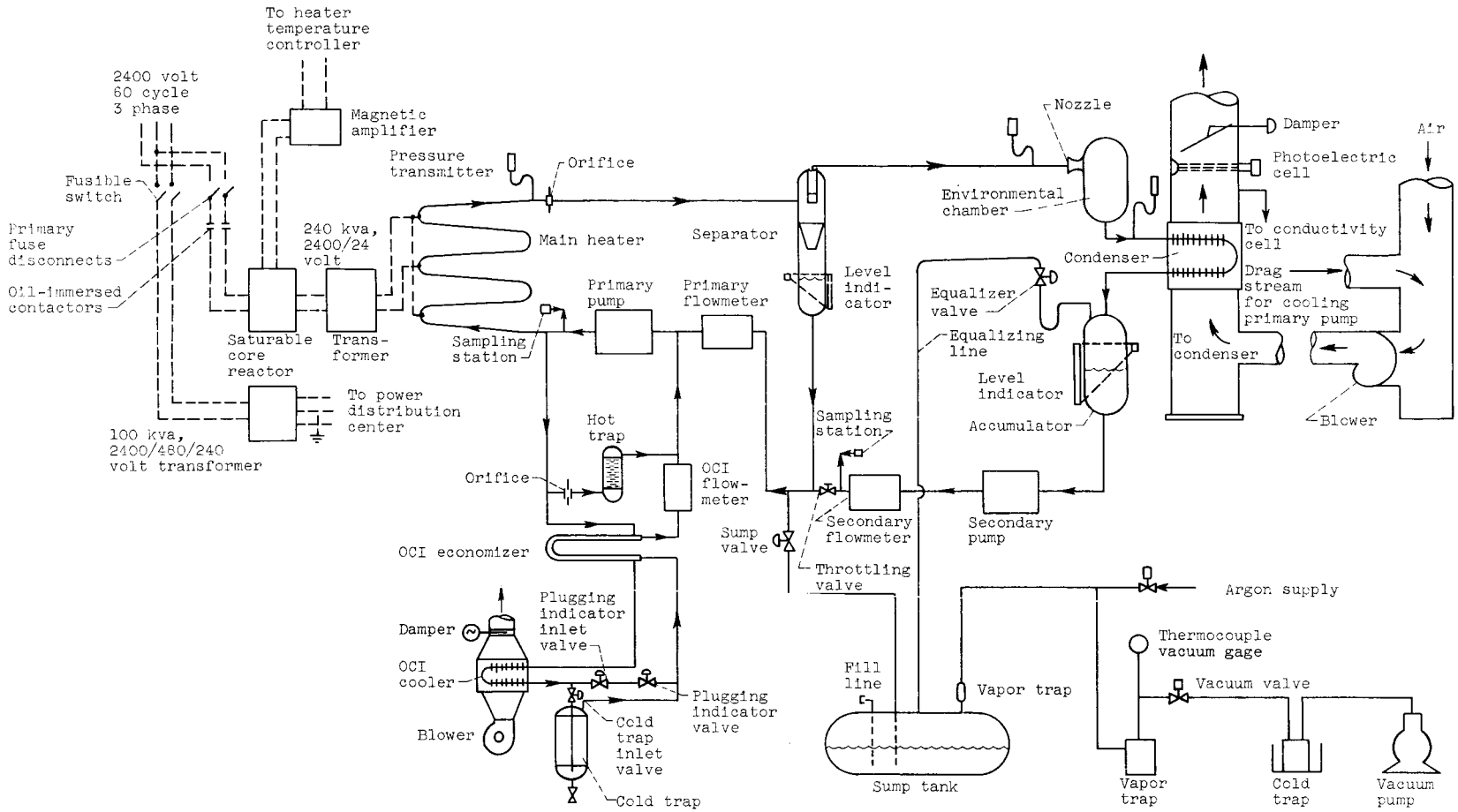

Figure 2. - Schematic drawing of sodium flash-vaporization facility.

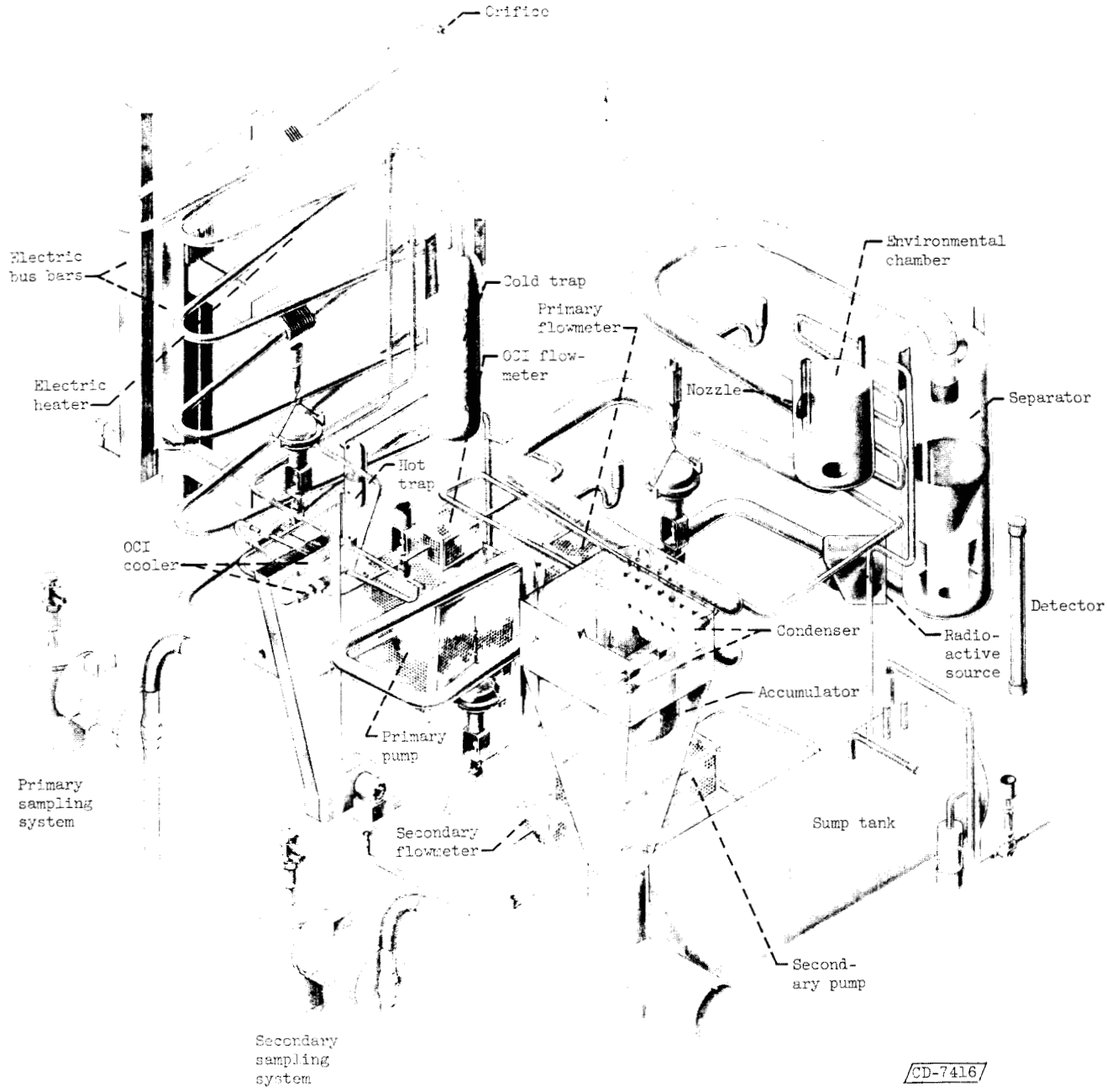

Figure 3. - Isometric drawing of sodium flash-vaporization facility.

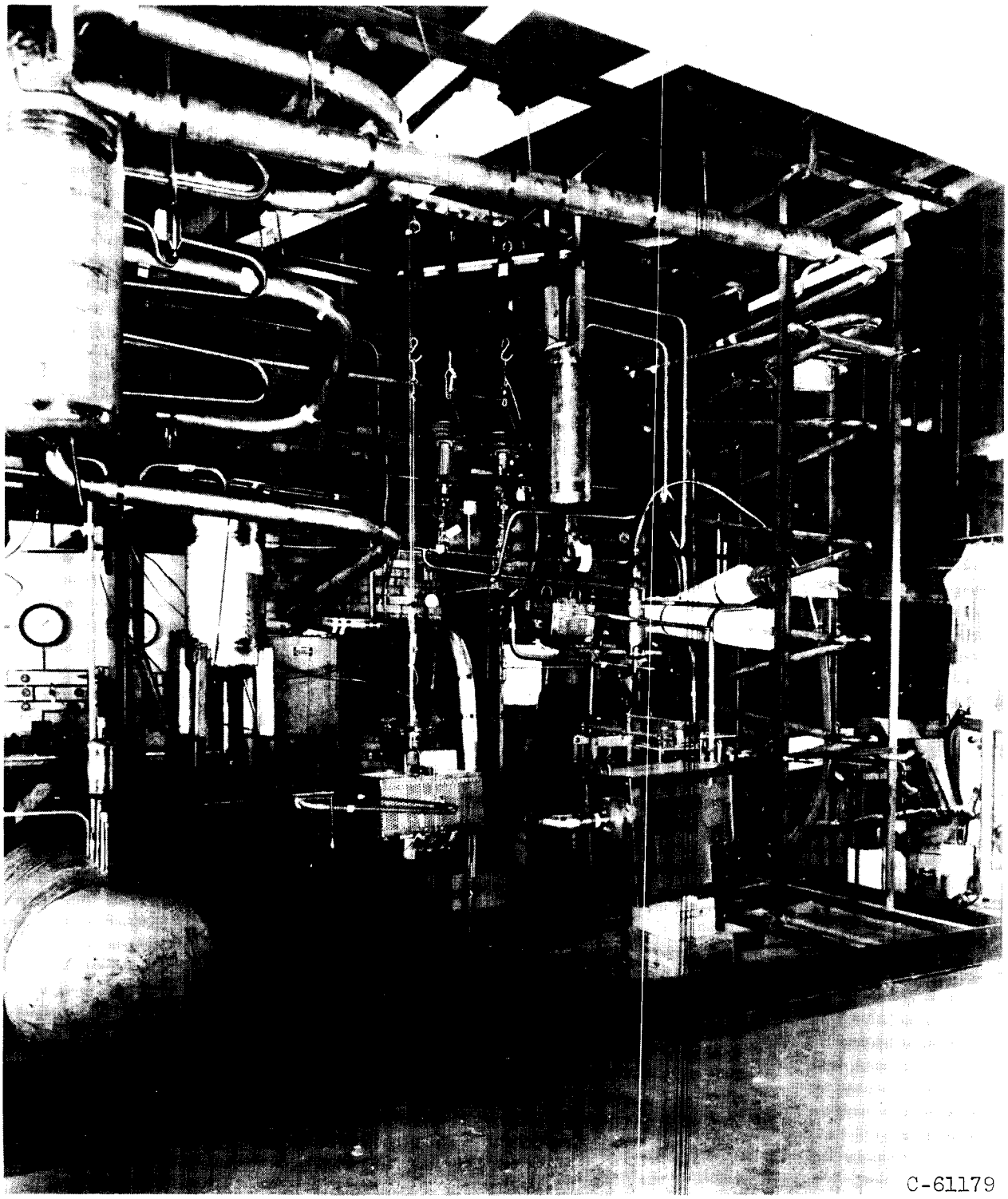

(a) During construction.

Figure 4. - Sodium flash-vaporization facility.

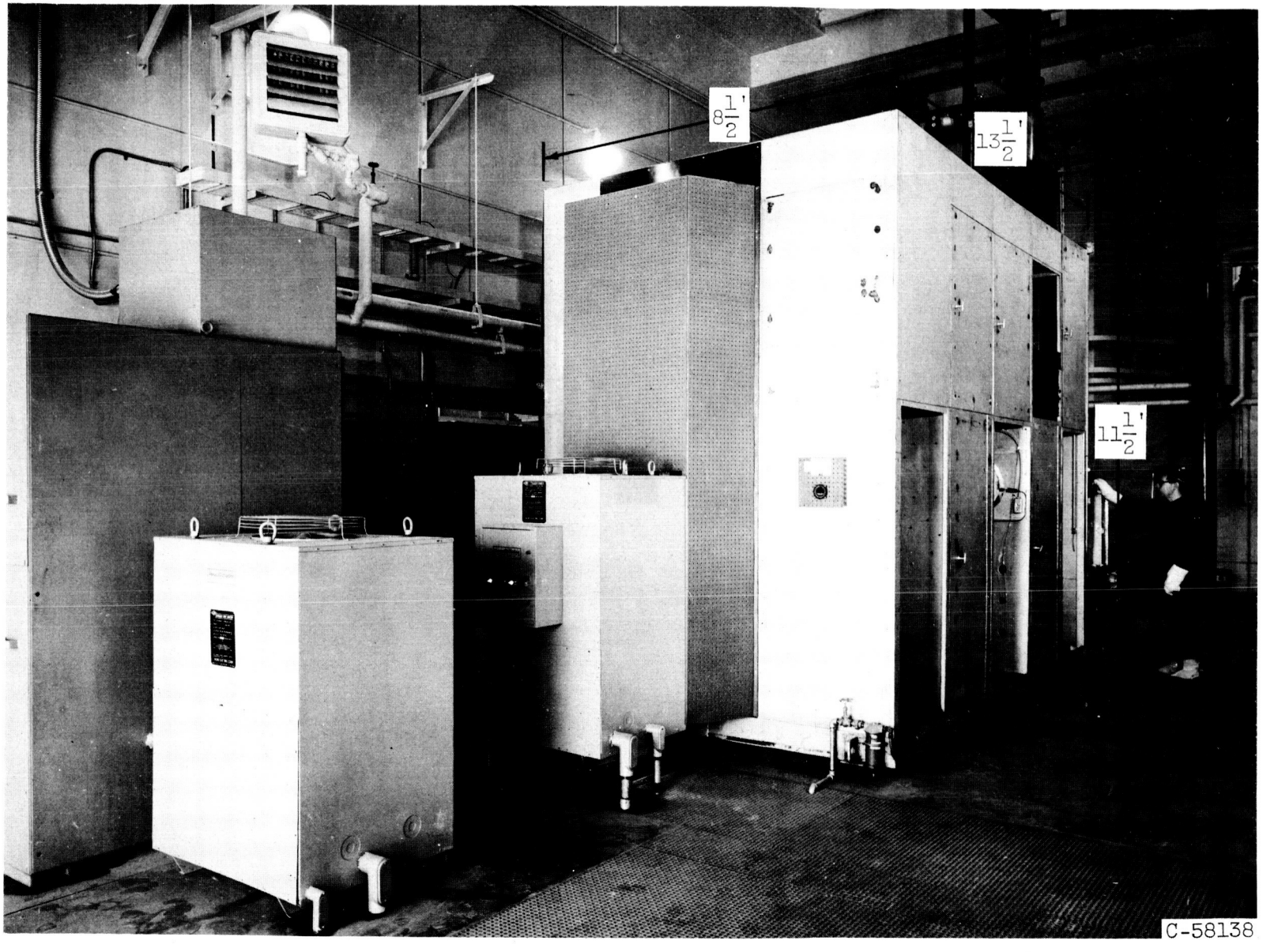

(b) After completion.

Figure 4. - Concluded. Sodium flash-vaporization facility.

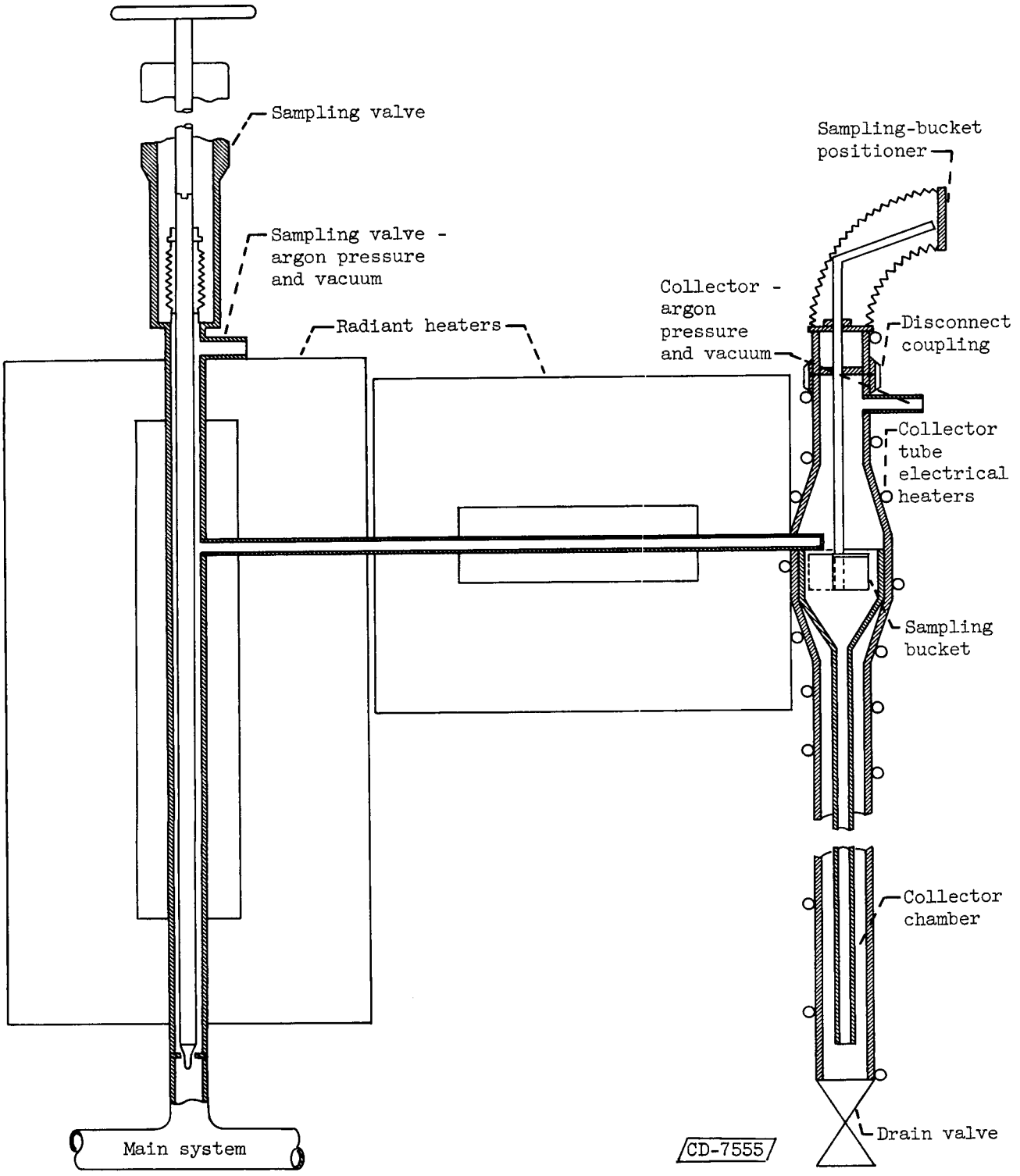

Figure 5. - Sampling system.

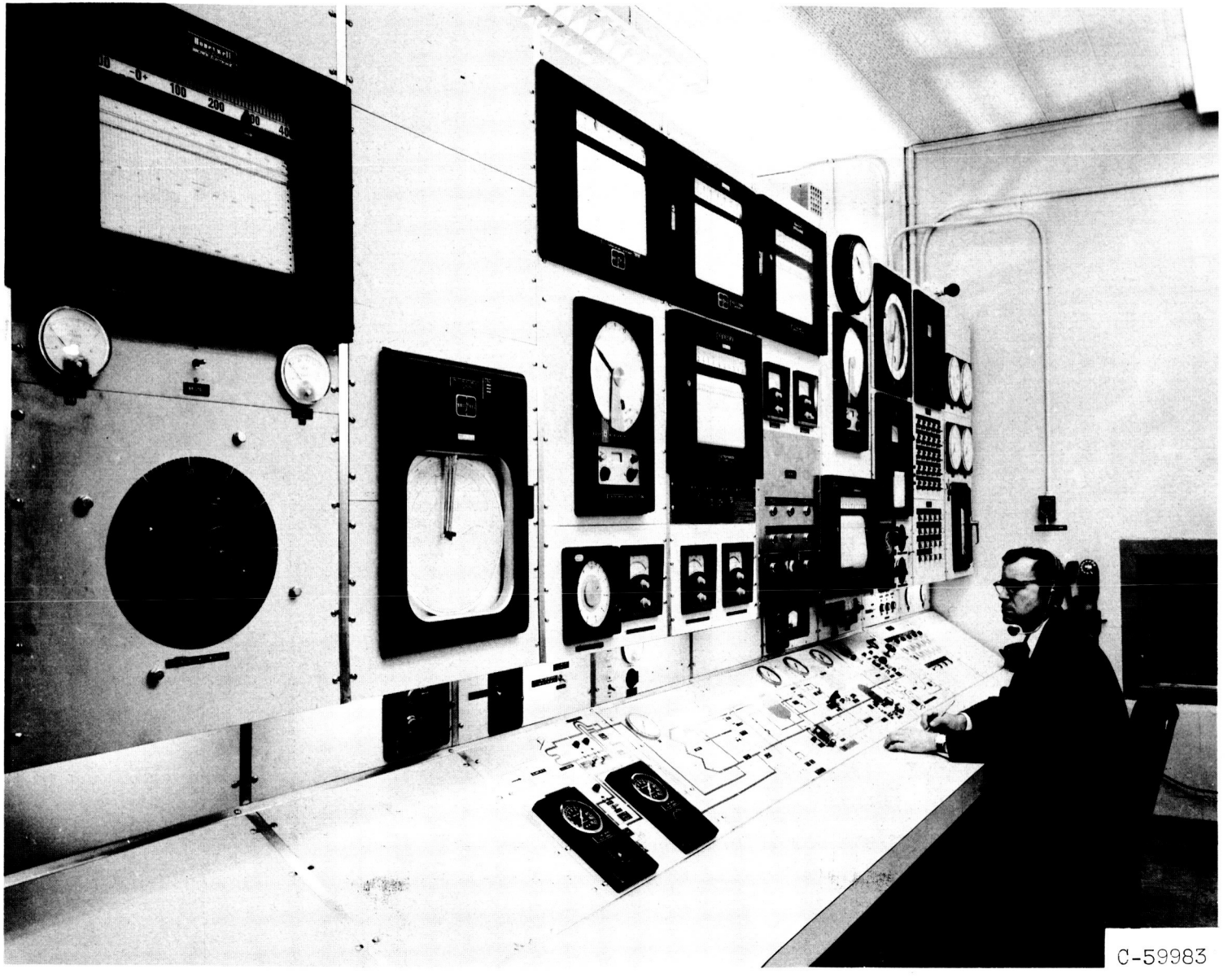

Figure 6. - Control room.

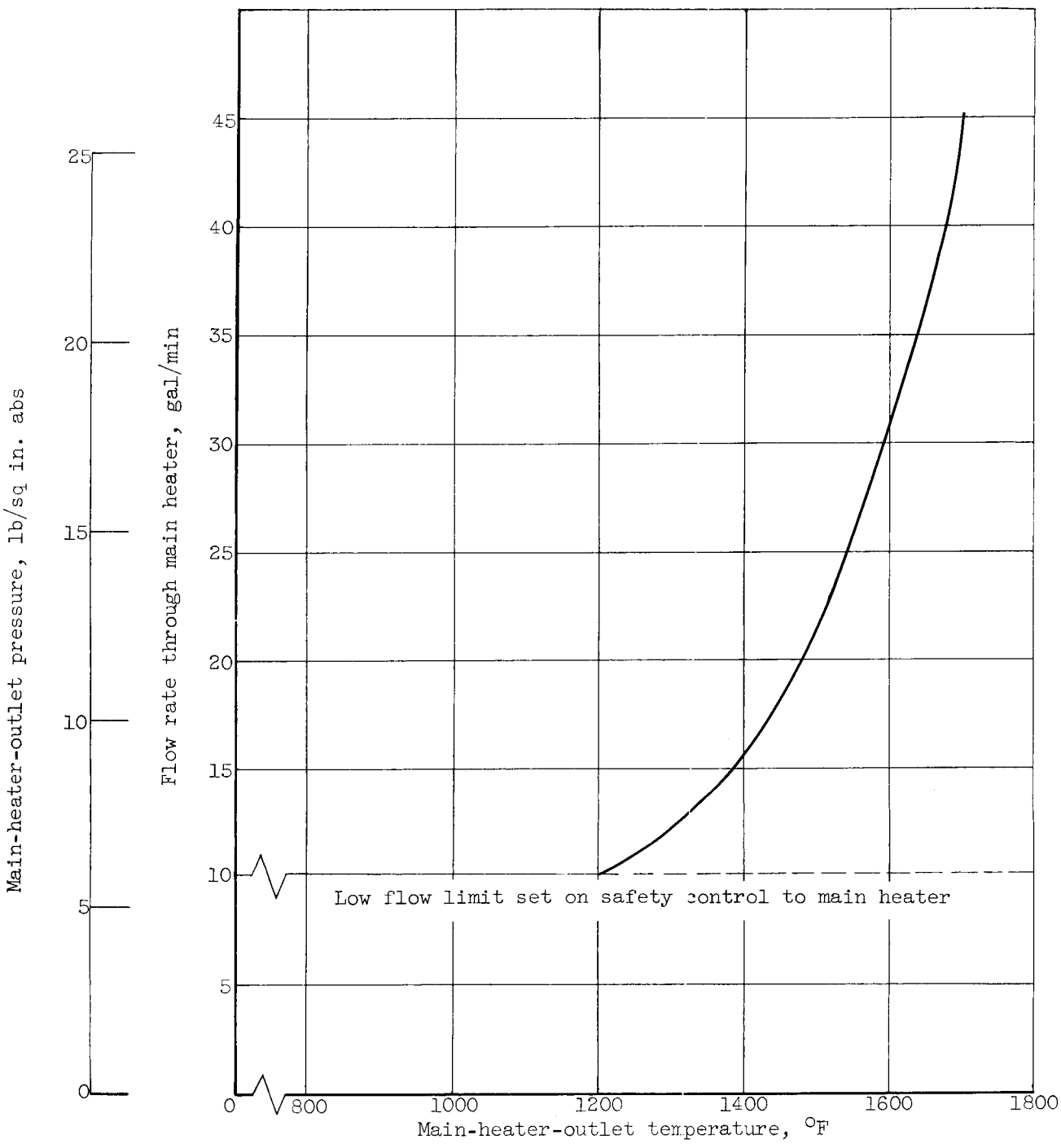

Figure 7. - Minimum permissible primary flow rate.

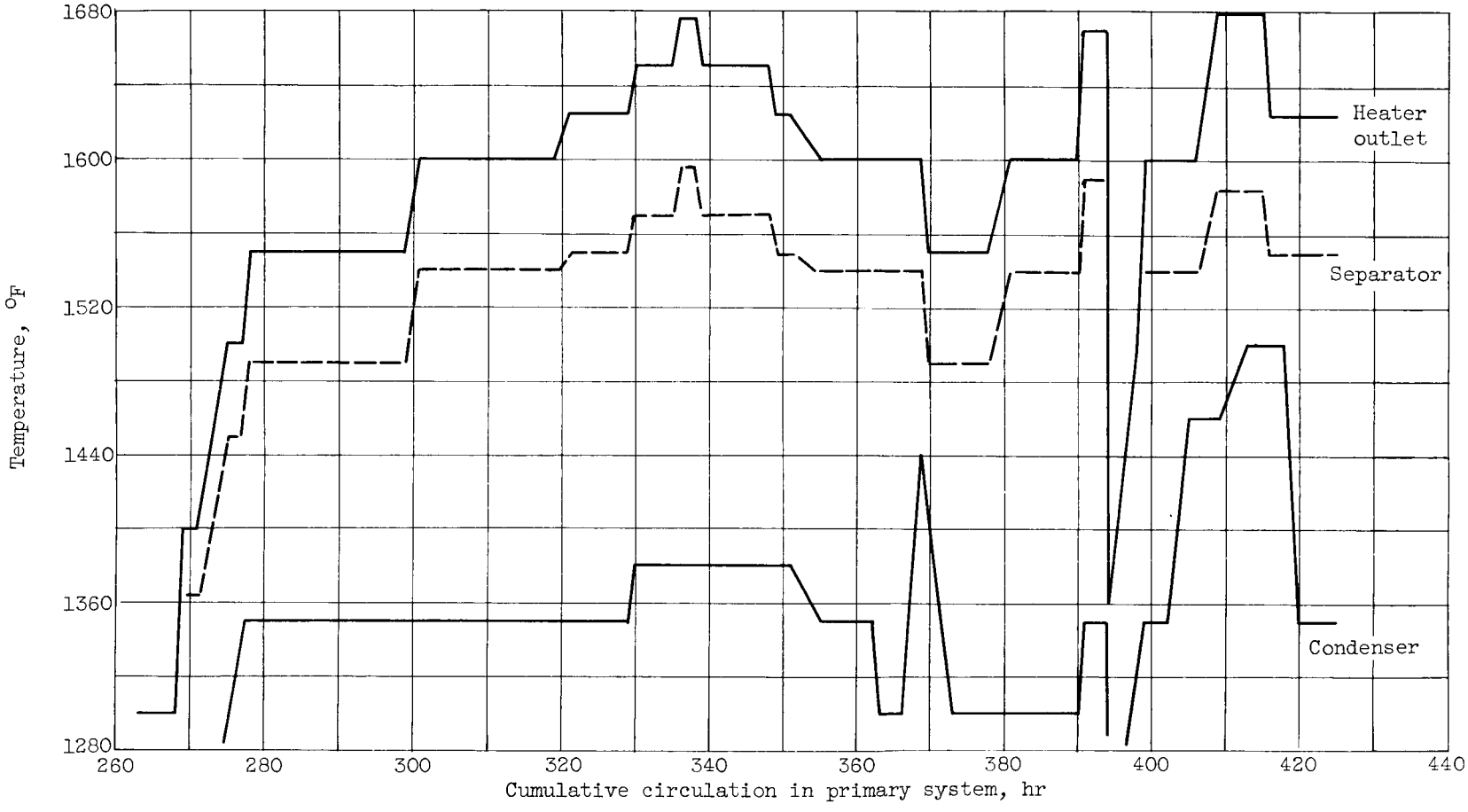

(a) First period.

Figure 8. - Operational performance of flash-vaporization facility for two uninterrupted 150-hour periods as a function of temperature.

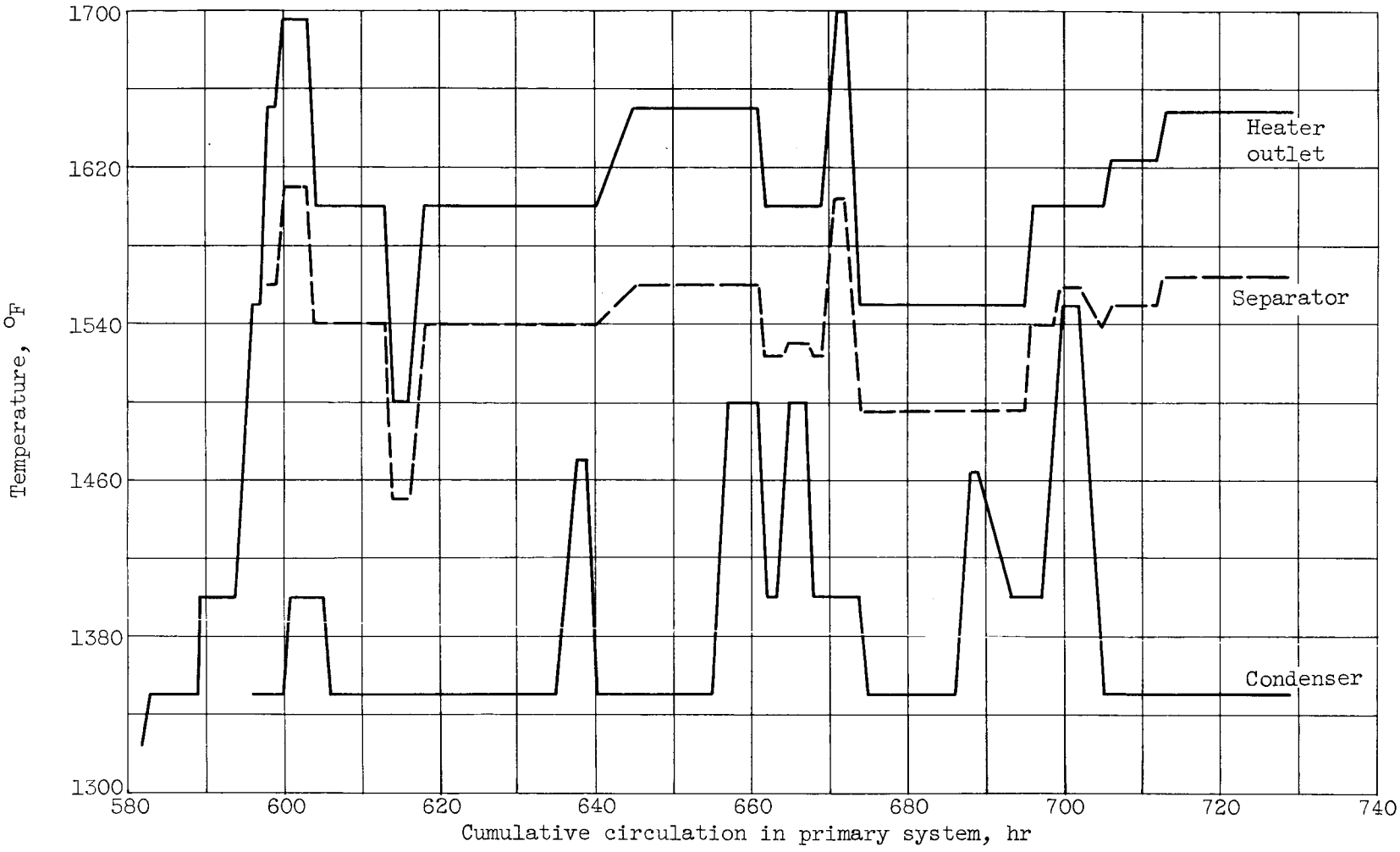

(b) Second period.

Figure 8. - Concluded. Operational performance of flash-vaporization facility for two uninterrupted 150-hour periods as a function of temperature.

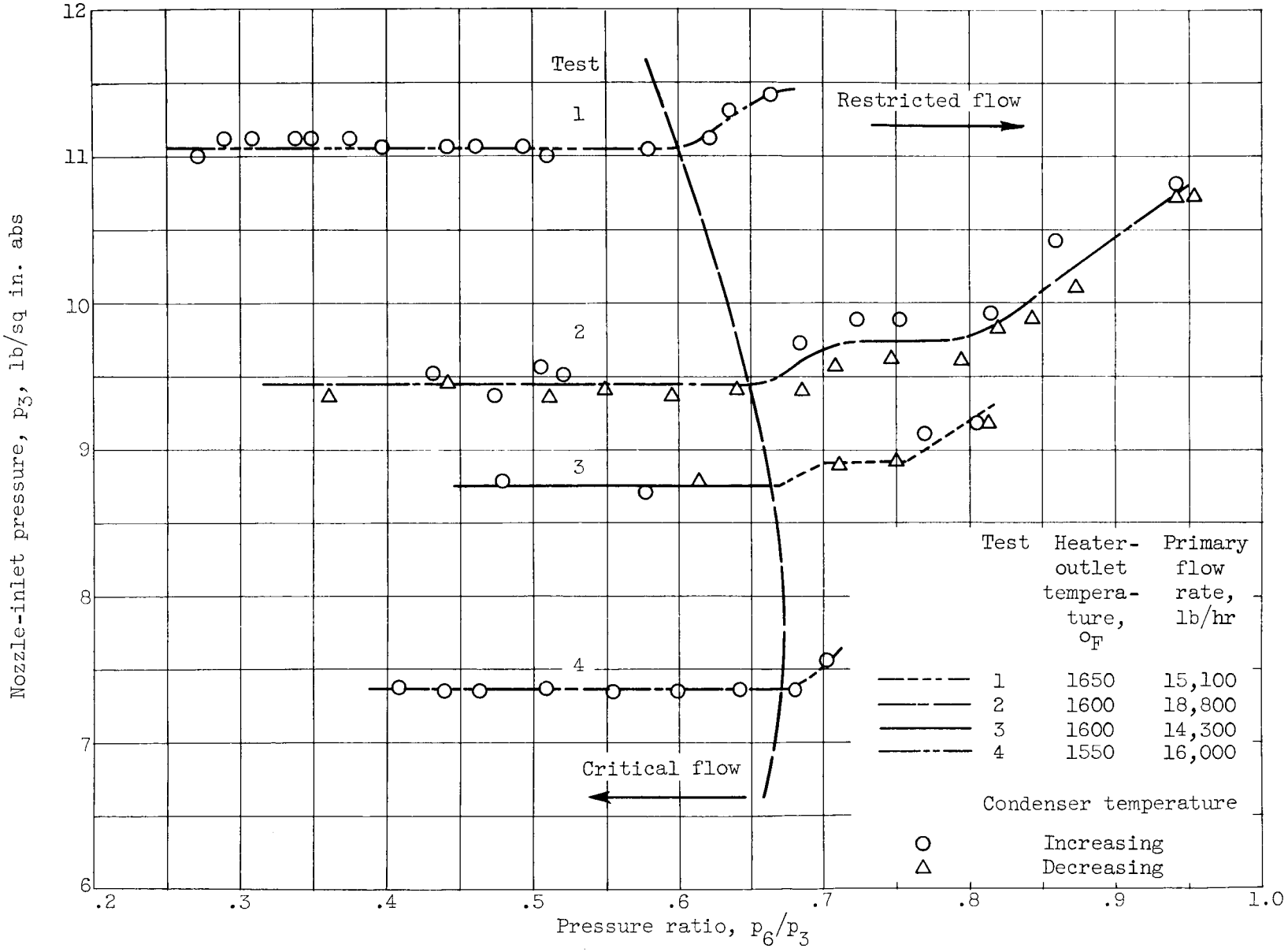

Figure 9. - Variation of nozzle-inlet pressure with ratio of condenser pressure to nozzle-inlet pressure.

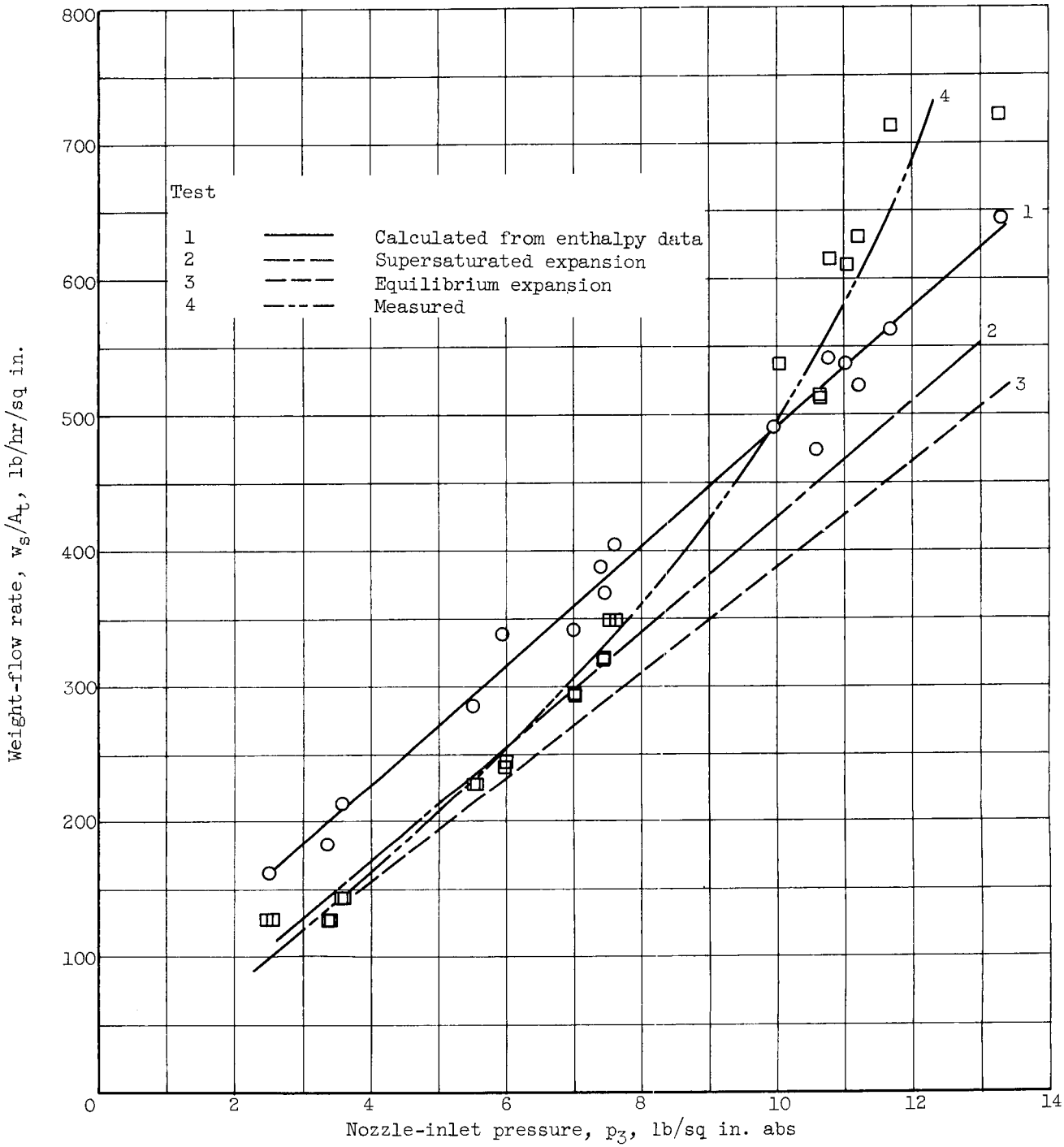

Figure 10. - Variation of critical weight-flow rate with nozzle-inlet pressure.

(a) External view.

Figure 11. - Weld failure of 1/2-inch pipe.

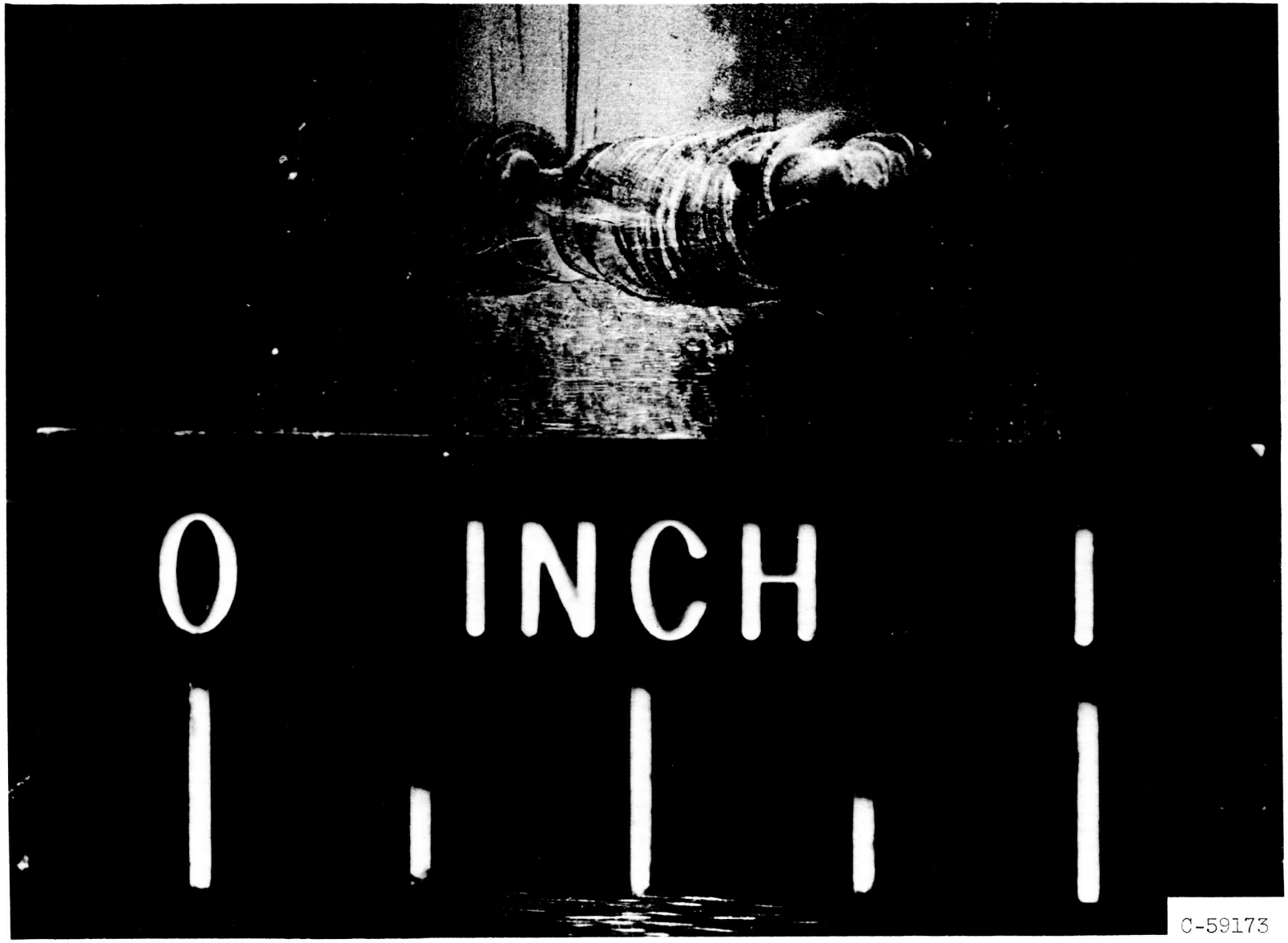

(b) Internal view.

Figure 11. - Concluded. Weld failure of 1/2-inch pipe.

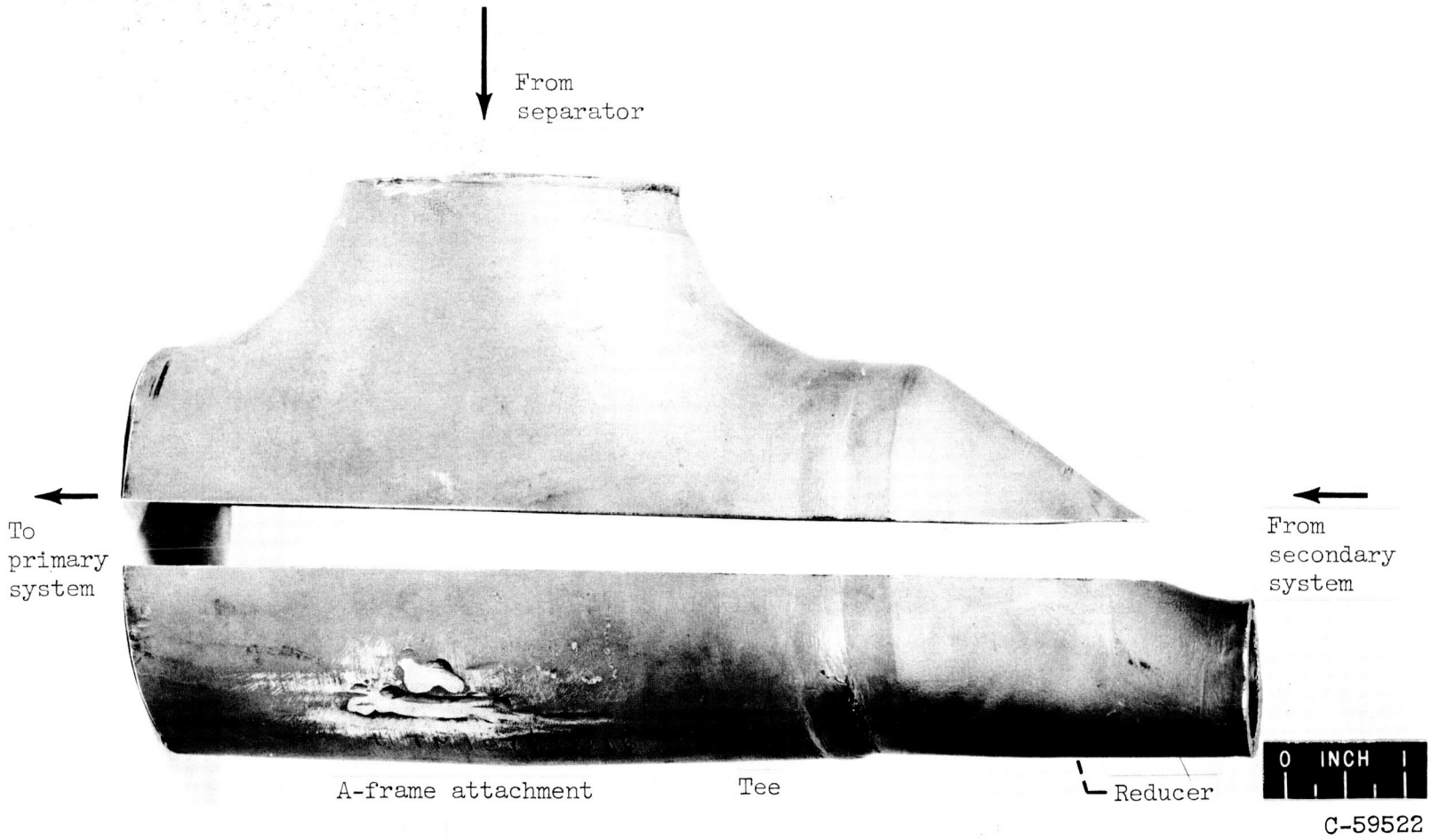

Figure 12. - Junction of primary and secondary systems.

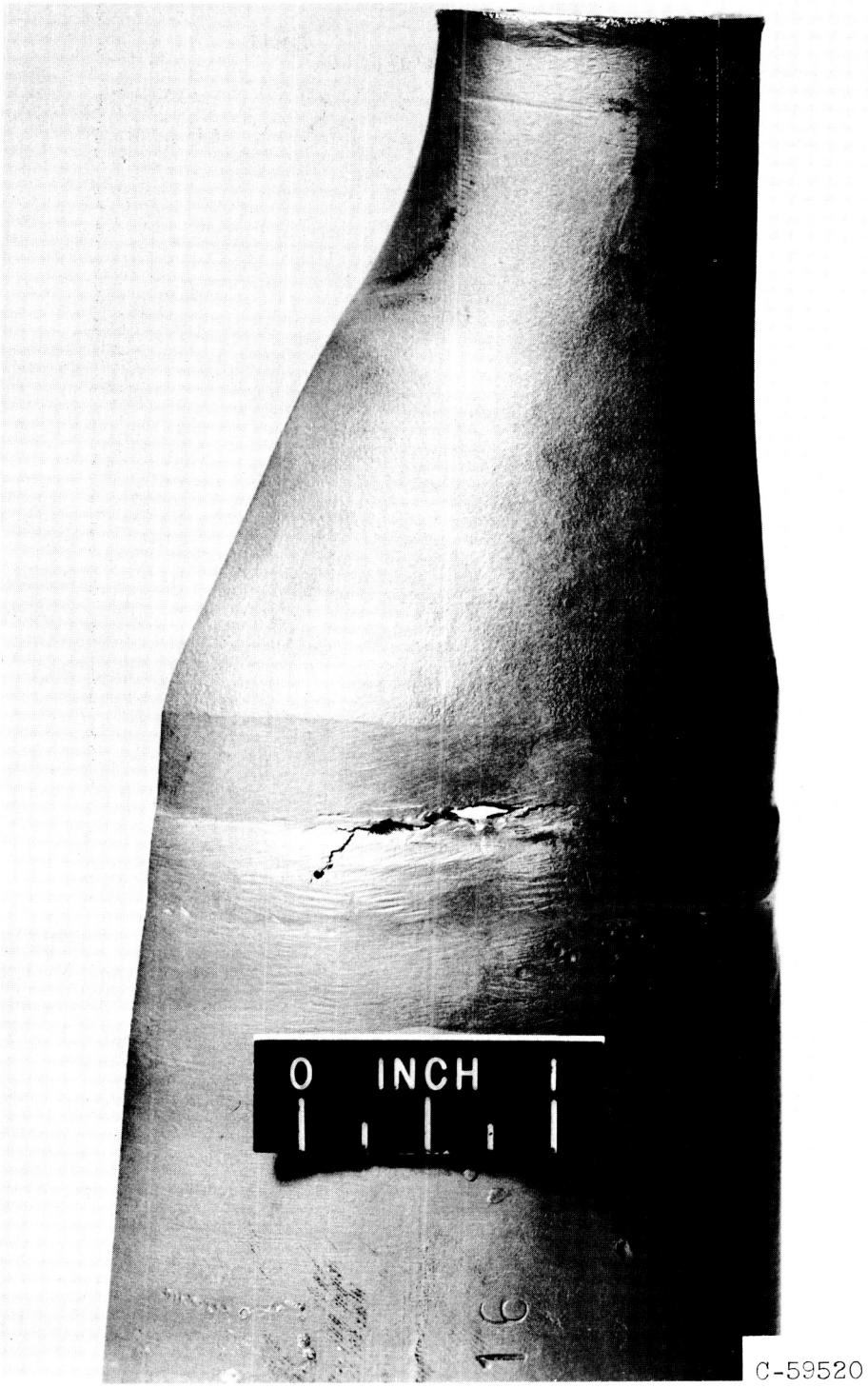

Figure 13. - Failure at primary and secondary junction.

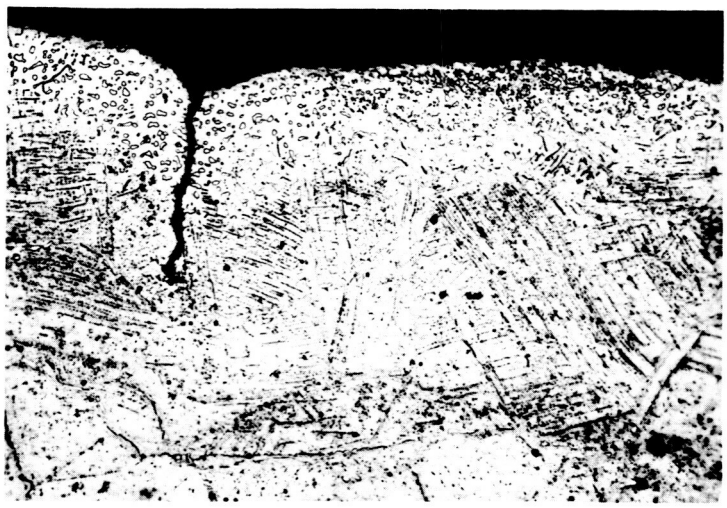

Figure 14. - Strains and excess carbide condition of reducer section near failure area. ×250.

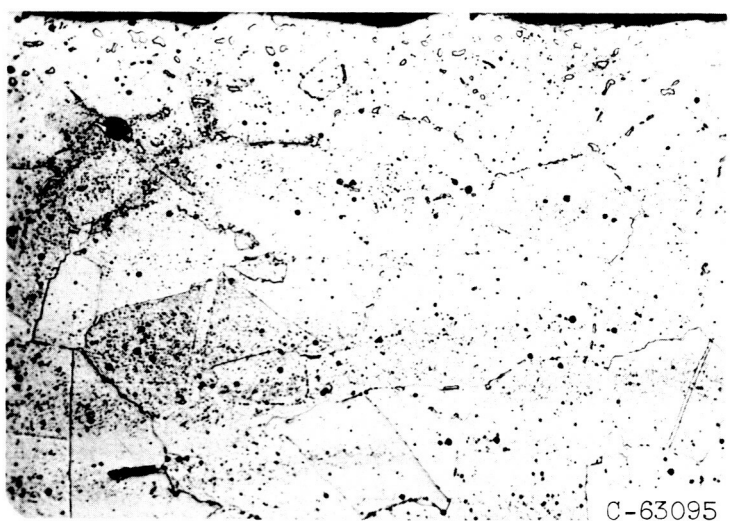

Figure 15. - Comparative area in $2\frac{1}{2}$-inch-diameter tee section near failure area.

Figure 16. - Strains and above average grain boundary carbide away from failure area (reducer section). ×250.

Figure 17. - Normal 316 stainless-steel structure away from failure area ($2\frac{1}{2}$-in.-diam. tee section.)

Figure 18. - Crack and carbide grain boundary segregation in weld root pass.

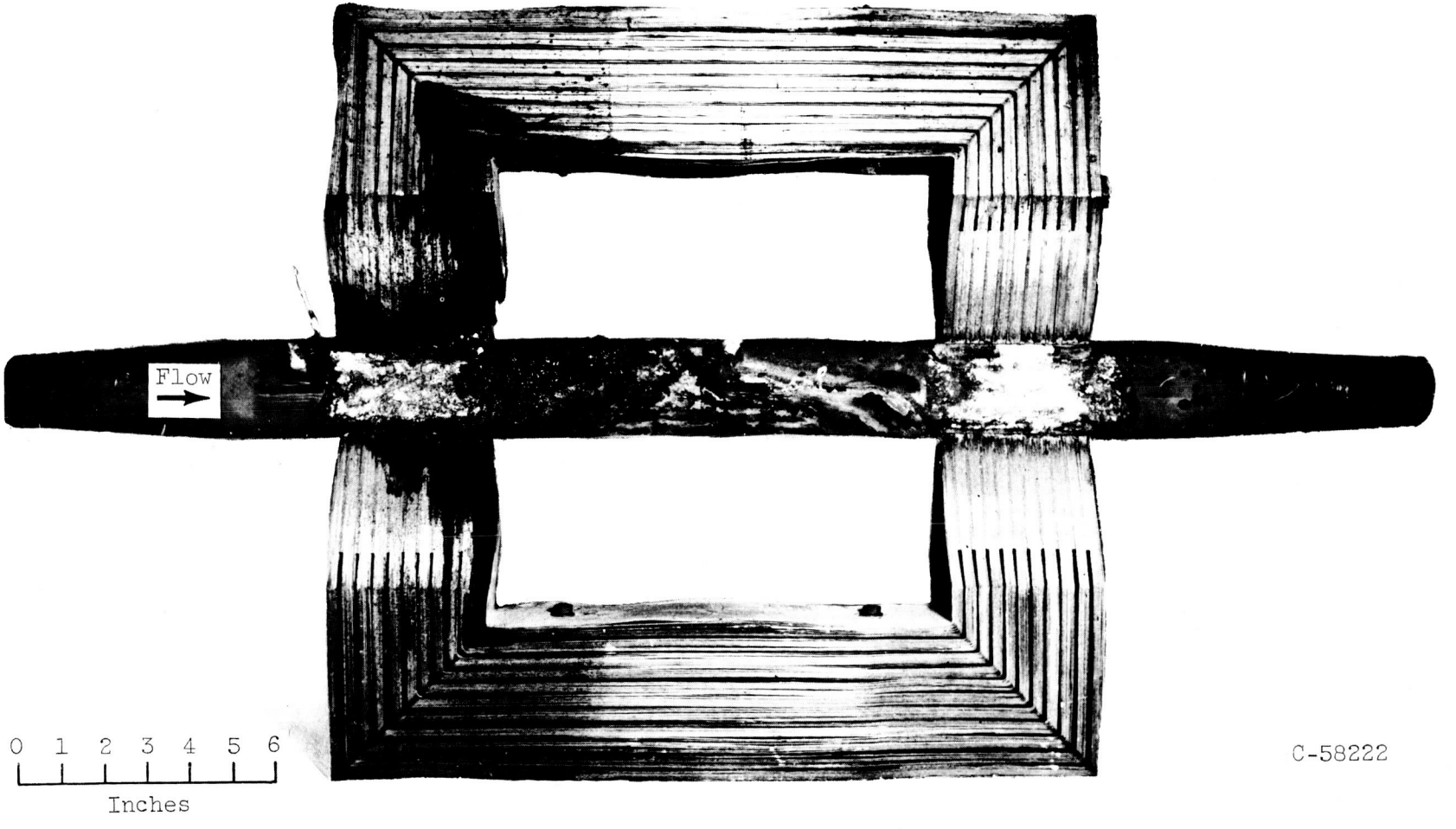

(a) Pumping tube with nickel bus bars attached.

Figure 19. - Pump A.

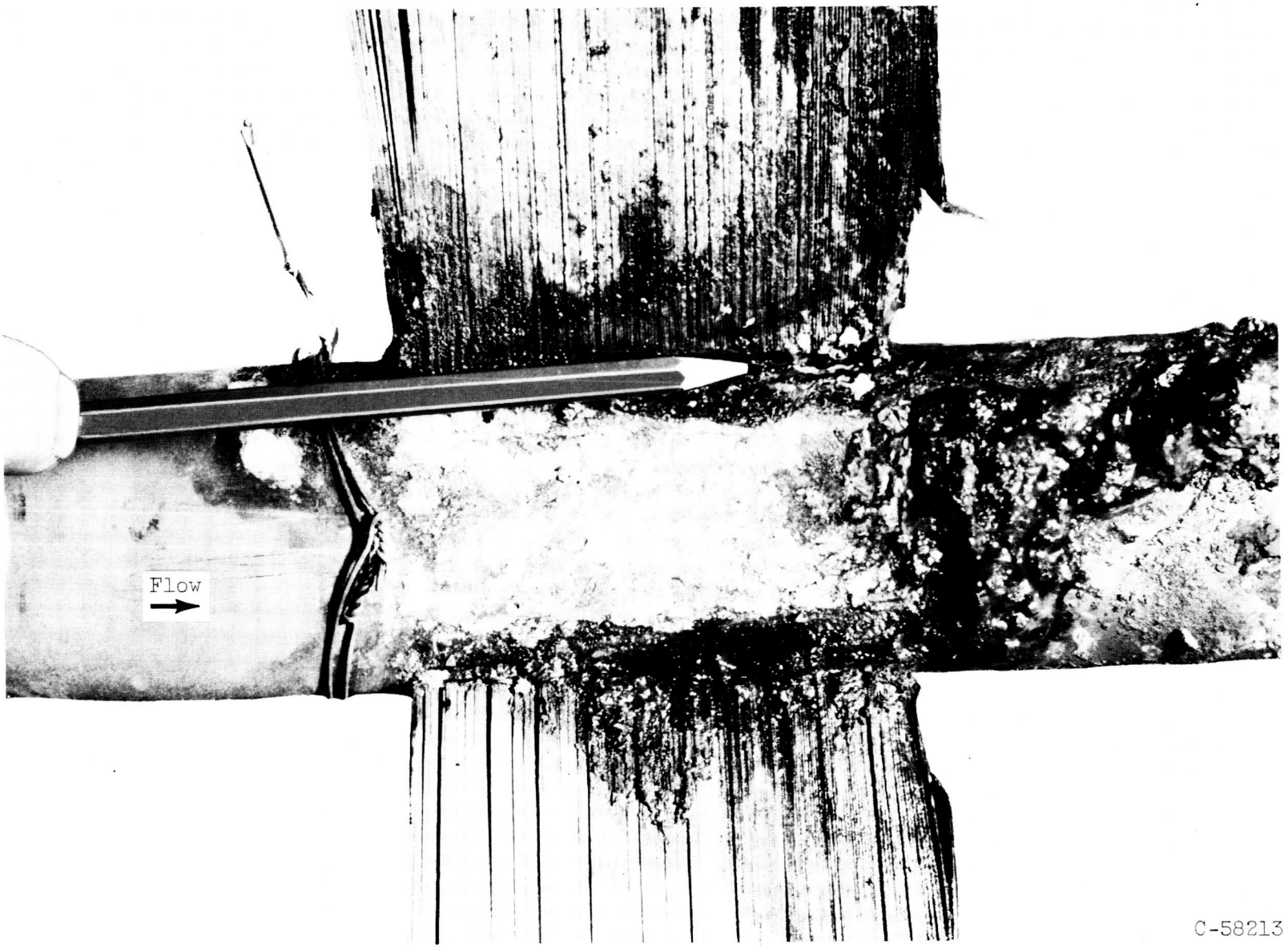

(b) Inlet pumping stage showing area of failure.

Figure 19. - Concluded. Pump A.

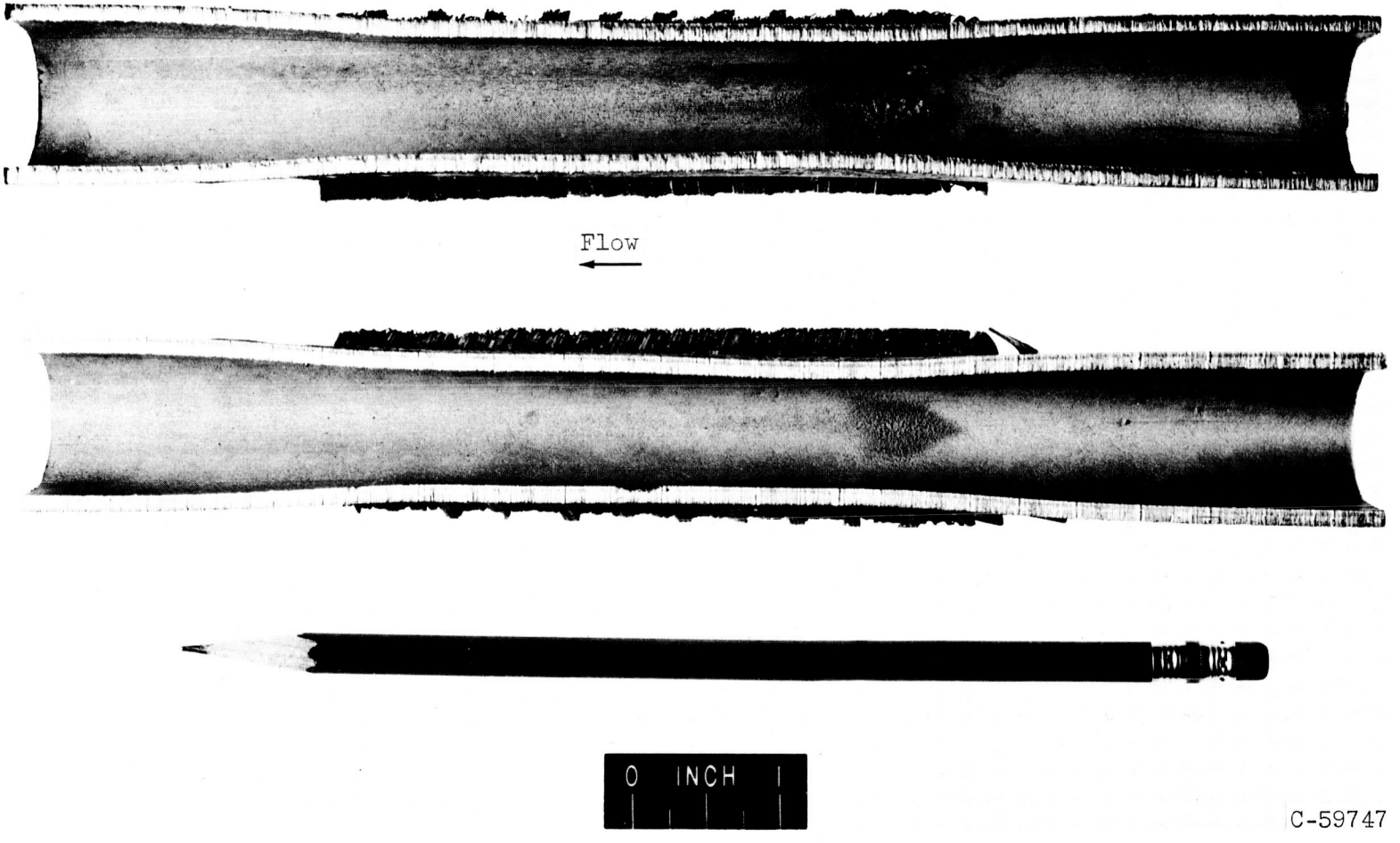

Figure 20. - Second pumping stage showing area of failure - pump B.

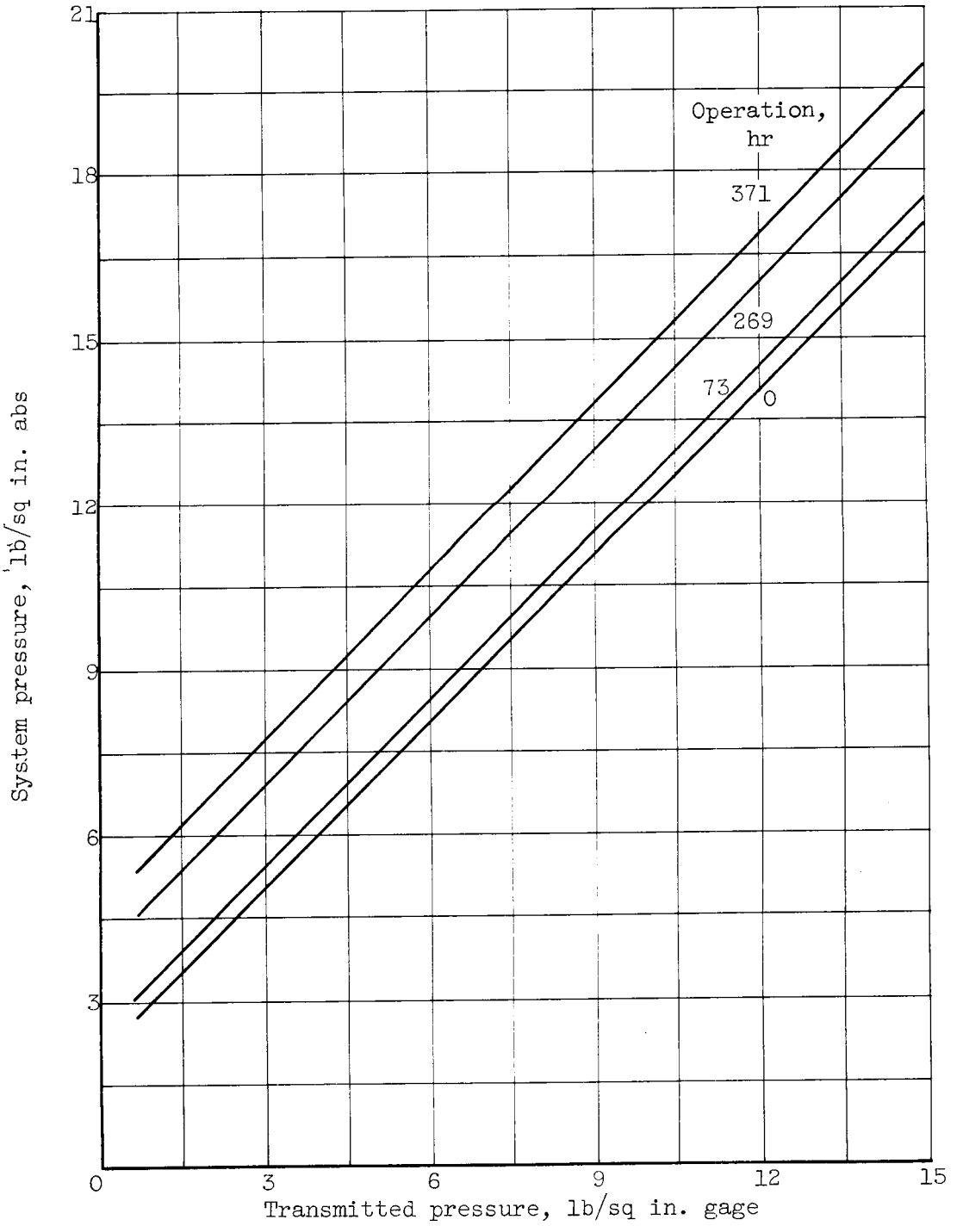

Figure 21. - Effect of time on pressure transmitter calibration for converging nozzle-inlet pressure transmitter. Transmitter temperature, 400° F.